

LLM Collusion

Shengyu Cao

Rotman School of Management, University of Toronto, shengyu.cao@rotman.utoronto.ca

Ming Hu

Rotman School of Management, University of Toronto, ming.hu@rotman.utoronto.ca

We investigate how the widespread adoption of large language models (LLMs) for pricing decisions can facilitate collusion among competing sellers. We develop a theoretical framework to analyze a duopoly in which both sellers delegate pricing to the same pre-trained LLM characterized by two parameters: a propensity parameter that captures the model's internal preference for high-price recommendations, and an output fidelity parameter that measures the alignment between this preference and the generated outputs. The LLM updates its propensity through retraining the model. Somewhat surprisingly, we find that the seemingly prudent practice of configuring LLMs for robustness and reproducibility in high-stakes pricing tasks gives rise to collusion through a phase transition. Specifically, we establish a critical output-fidelity threshold that governs long-run market behavior. Below this threshold, competitive pricing is the unique long-run outcome regardless of initial conditions. Above this threshold, the system exhibits bistability, with both competitive and collusive pricing being locally stable, and the realized outcome is determined by the model's initial preference. The collusive pricing outcome resembles tacit collusion: prices are elevated on average, but occasional low-price recommendations create plausible deniability and prevent detection. When output fidelity is perfect, full collusion emerges from any interior starting point. Moreover, for finite training batches with batch size b , we show that infrequent model retraining, driven by computational costs, further amplifies collusion. Specifically, when the initial preference lies in the region that leads to collusive pricing, the probability of collusion approaches one as batch size increases, as larger batches suppress stochastic fluctuations that might otherwise drive the system toward competitive pricing. The region of indeterminate outcomes shrinks at a rate of $O(1/\sqrt{b})$, so that larger batches convert more initial conditions into predictably collusive trajectories.

1. Introduction

The rapid adoption of algorithms in commercial decision-making has attracted increasing regulatory scrutiny. In March 2024, the Federal Trade Commission (FTC) and the Department of Justice (DOJ) issued a joint statement warning that algorithmic pricing systems can facilitate illegal collu-

sion, even in the absence of explicit agreements among competitors.¹ Subsequent enforcement signals have only intensified: in August 2025, DOJ Assistant Attorney General Gail Slater announced that algorithmic pricing investigations would significantly increase as deployment of the technology becomes more prevalent.²

This regulatory concern is particularly salient as sellers increasingly rely on large language models (LLMs) for pricing decisions, an area the regulation has not yet addressed. A 2024 McKinsey survey of Fortune 500 retail executives found that 90% have begun experimenting with generative AI solutions, with pricing and promotion optimization emerging as a priority use case.³ In Europe, 55% of retailers plan to pilot generative AI-based dynamic pricing by 2025, building on the 61% who have already adopted some form of algorithmic pricing.⁴ Industry applications are already operational: Wang et al. (2025) report that Alibaba has deployed an LLM-based pricing system on its Xianyu platform to provide real-time price recommendations for sellers.

This heightened regulatory pressure coincides with remarkable market concentration in the LLM industry. As of 2025, ChatGPT commands approximately 62.5% of the business-to-consumer AI subscription market, while 92% of Fortune 500 companies report using OpenAI products.⁵ This confluence of concentrated AI infrastructure and heightened antitrust concern raises a fundamental question: Can the widespread adoption of LLMs for pricing decisions facilitate collusion across competing sellers?

The possibility that algorithms might learn to collude has been studied extensively in the context of machine learning/reinforcement learning (RL). Banchio and Mantegazza (2022) demonstrate that Q-learning agents can converge to supracompetitive prices in repeated games through trial-and-error learning. However, such collusion typically requires extensive training periods and millions of interactions, providing some reassurance that computational barriers might limit practical concern. LLMs present a fundamentally different paradigm. Unlike RL agents that learn pricing strategies from scratch through repeated market interactions, LLMs arrive pretrained on vast corpora of human knowledge, including business strategy, economic theory, and pricing practices.

¹ FTC Press Release, “FTC and DOJ File Statement of Interest in Hotel Room Algorithmic Price-Fixing Case,” March 28, 2024.

² MLex Market Insight, “Algorithmic pricing probes to increase as use grows, US DOJ’s Slater says,” August 11, 2025.

³ McKinsey & Company, “LLM to ROI: How to Scale Gen AI in Retail,” April 2024.

⁴ Valcon, “Dynamic Pricing Predictions for 2025,” January 2025.

⁵ Data from Earnest Analytics via Backlinko, “ChatGPT Statistics 2025,” available at <https://backlinko.com/chatgpt-stats>. The Fortune 500 statistic was announced by OpenAI in April 2024.

Recent experimental work by Fish et al. (2024) documents that LLM-based pricing agents converge to suprarevenue prices much more rapidly than their RL counterparts: GPT-4 agents reach near-optimal collusive pricing within 100 periods, compared to the hundreds of thousands to millions of periods required for Q-learning algorithms. Yet the theoretical mechanisms underlying this acceleration remain poorly understood.

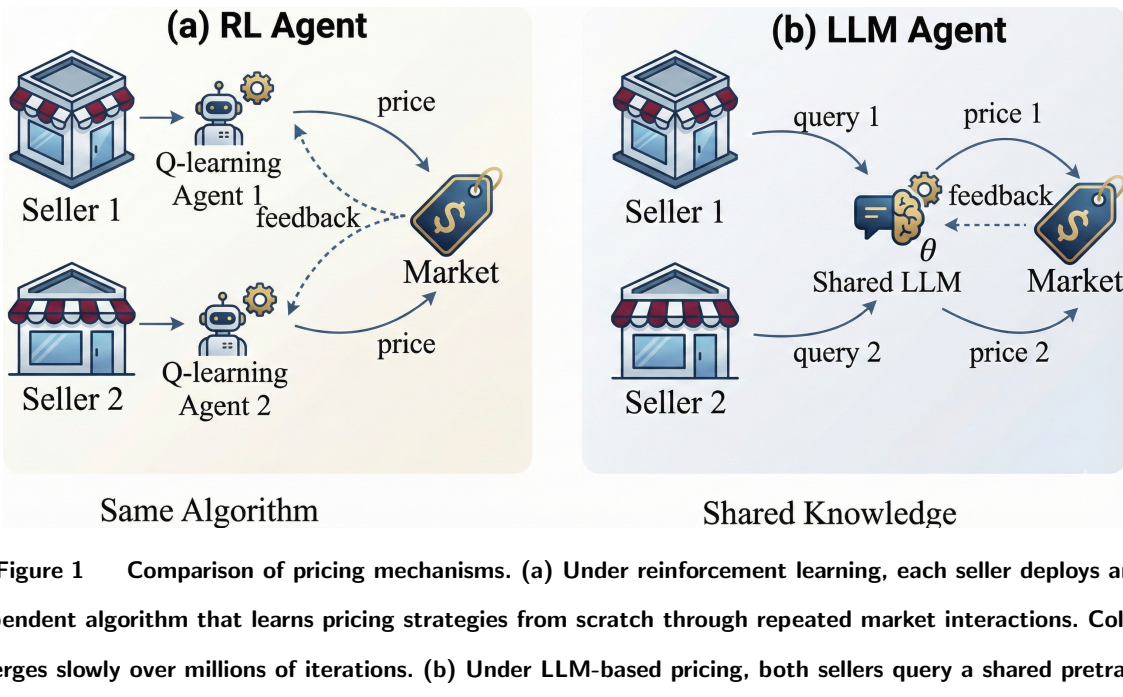


Figure 1 Comparison of pricing mechanisms. (a) Under reinforcement learning, each seller deploys an independent algorithm that learns pricing strategies from scratch through repeated market interactions. Collusion emerges slowly over millions of iterations. (b) Under LLM-based pricing, both sellers query a shared pretrained model with a latent high-price preference θ . The shared knowledge infrastructure creates correlated recommendations, while data sharing during retraining aggregates seller feedback, forming a self-reinforcing loop that drives rapid convergence to collusive outcomes.

We identify two sources of collusion risk unique to LLM-based decision-making and illustrate the contrast between LLM-based and RL-based approaches in Figure 1. Specifically, the first source is the *shared knowledge* infrastructure that arises from market concentration. Given the dominant position documented above, competing sellers frequently delegate pricing decisions to the same LLM provider. When multiple sellers query the same model, their adopted recommendations may become correlated through the model’s internal latent preferences, a structural tendency toward certain pricing strategies encoded in its weights. This correlation creates implicit coordination without any communication between sellers: even if each seller queries the LLM independently, the common underlying preference induces positive correlation in their pricing actions. Moreover, shared knowledge persists even when sellers use different LLM providers. Leading LLMs are often

distilled into smaller models by competitors, transferring embedded pricing heuristics from dominant providers to the broader ecosystem.⁶ In addition, pretraining corpora across providers draw from largely overlapping public sources, including business literature, economic textbooks, and strategic discussions that extensively document the profitability of coordinated pricing. Alignment procedures such as reinforcement learning from human feedback (RLHF) further homogenize model behavior, as evaluators or users at different companies apply similar standards of “helpfulness” and “reasonableness.” This raises a fundamental question: Does shared knowledge infrastructure, whether through common providers or homogenized training, lead to correlated pricing recommendations that translate into market-level collusion?

The second source of risk is the *data sharing* policies that govern model improvement. Major LLM providers collect user interaction data to refine their models, creating feedback loops between seller behavior and model updates. Google’s Gemini, for instance, uses a “Keep Activity” setting that is enabled by default for users aged 18 and over, allowing the platform to analyze conversations and use uploaded files, images, and videos for AI training.⁷ Anthropic’s August 2025 policy change similarly made data sharing the default setting, with five-year retention for users who consent.⁸ xAI offers \$150 in monthly API credits to developers who share their interaction data, with no mechanism to opt out once the program is joined.⁹ When multiple sellers share their pricing interactions and outcomes with the same LLM provider, the model’s retraining process aggregates this data. A model that observes high prices leading to high profits across multiple sellers may update its preferences accordingly. This raises another fundamental question: Does data aggregation from competing sellers create a self-reinforcing feedback loop that drives prices toward collusive levels?

This paper develops a theoretical framework to analyze the emergence of collusion when sellers delegate pricing decisions to the same LLM, addressing these two questions. Surprisingly, we find that collusion can emerge as an unintended consequence of standard operational practices. In high-stakes tasks such as pricing, decision-makers typically configure LLMs for robustness and reproducibility by setting decoding temperatures to zero or near-zero. This seemingly prudent choice increases the correlation between the model’s internal preference and its generated outputs,

⁶ For instance, many open-source models such as LLaMA derivatives are trained to mimic the outputs of frontier models like GPT-4.

⁷ Google Privacy Policy update, June 2025. Data is “reviewed by trained service providers and used to improve Google services (including Gemini models and other generative AI models).”

⁸ TechCrunch, “Anthropic users face a new choice – opt out or share your chats for AI training,” August 28, 2025. See also Anthropic’s official announcement at <https://www.anthropic.com/news/updates-to-our-consumer-terms>.

⁹ xAI Data Sharing Program terms specify that “after a team has chosen to opt-in to data sharing, the team cannot opt-out.”

thereby facilitating coordination without explicit communication. Moreover, infrequent retraining schedules necessitated by prohibitively high computational costs further amplify the risk of collusion. Major LLM providers typically release model updates every 6–12 months, translating into large effective batch sizes that suppress the beneficial noise which might otherwise allow prices to escape to competitive levels.

Model. We consider a symmetric duopoly pricing game in which two sellers compete by simultaneously choosing between a high-price strategy (H) and a low-price strategy (L). Both sellers delegate their pricing decisions to the same LLM. The LLM’s behavior is characterized by two parameters: a *propensity parameter* $\theta \in [0, 1]$ representing the model’s internal preference for high-price recommendations, and an *output fidelity* $\rho \in [0.5, 1]$ capturing the alignment probability between this preference and the generated output. The LLM updates its propensity through model retraining: after observing actions and outcomes over every batch of $b \geq 1$ decision rounds, the model evaluates the relative performance of high-price versus low-price recommendations and adjusts θ accordingly. This update follows a log-odds recursion that increases θ when high prices outperform and decreases it otherwise.

Results. We first analyze a benchmark setting in which the LLM retraining is performed on large batches of interaction data, so that estimation noise becomes negligible. We show that whether high-price recommendations become self-reinforcing depends on two competing forces: the benefit of coordination when both sellers receive and follow the same high-price recommendation, versus the cost of miscoordination when sellers receive different recommendations and the low-price seller captures the market. When output fidelity is sufficiently high, coordination benefits dominate, and learning reinforces the LLM’s preference for high prices.

It is worth noting that high output fidelity is precisely what decision-makers seek in practice. Low fidelity, corresponding to high-temperature decoding, introduces randomness into recommendations. Such unpredictability imposes operational costs on sellers: inconsistent pricing confuses customers and erodes brand equity, noisy outputs obscure whether realized profits stem from sound strategy or mere chance, and stochastic recommendations undermine the explainability that regulators increasingly demand of algorithmic pricing systems. Consequently, sellers naturally configure LLMs for robustness and reproducibility by setting decoding temperatures to zero or near-zero, which pushes output fidelity to high levels.

We establish a phase transition in long-run pricing behavior, governed by a critical output-fidelity threshold. Below this threshold, competitive pricing is the unique stable outcome: the LLM

converges to recommending low prices regardless of its initial preference. Above this threshold, two stable outcomes coexist: competitive pricing and collusive pricing. Which outcome is realized depends on the model’s initial preference. When output fidelity is perfect, meaning the LLM’s recommendations perfectly reflect its internal preference, the system converges to full collusion from any interior starting point. The standard practice of configuring LLMs for reliability thus inadvertently pushes sellers into the parameter region where collusion can emerge.

We then analyze a more realistic setting in which the LLM is retrained on finite batches, so that randomness persists throughout learning. We show that the system still converges to a stable outcome, but which outcome is reached now depends on the random training data encountered along the way. Identical models with identical initial conditions can reach different long-run outcomes. We characterize how the probability of collusion depends on batch size and initial conditions. When the model’s initial preference lies in the region that leads to collusive pricing, larger batch sizes increase the probability of collusion by suppressing random fluctuations that might otherwise push the system toward competitive pricing. The zone of genuine uncertainty, where either outcome is possible, shrinks as batch size increases. This result implies that the infrequent retraining schedules adopted by major LLM providers, driven by computational costs, inadvertently amplify the risk of collusion by creating large effective batch sizes.

2. Literature Review

Our work is closely related to three streams of literature: algorithmic collusion, LLM-based pricing and strategic behavior, and algorithmic monoculture.

Algorithmic collusion. A growing body of research demonstrates that pricing algorithms can learn to sustain supra-competitive prices without explicit coordination (see [Bichler et al. 2025](#) for a review of the literature on algorithmic collusion). [Cooper et al. \(2015\)](#) analyze sellers using demand models that ignore competition, showing that learning dynamics can yield outcomes ranging from Nash equilibrium to collusive prices depending on model specification and initial conditions. [Calvano et al. \(2020\)](#) show that Q-learning algorithms in repeated pricing games converge to collusive outcomes through reward-punishment strategies. [Klein \(2021\)](#) extends this to sequential pricing, and [Banchio and Mantegazza \(2022\)](#) provide theoretical foundations by showing how independent algorithms can develop correlated beliefs that sustain collusion. [Hansen et al. \(2021\)](#) demonstrate that collusion can emerge through correlated pricing experiments, even when algorithms do not observe competitor prices. Empirically, [Assad et al. \(2024\)](#) document that margins in German retail gasoline markets increased by 28% when both duopoly competitors adopted algorithmic pricing.

The extent and robustness of algorithmic collusion remain debated. [Abada and Lambin \(2023\)](#) extend the framework to dynamic settings with imperfect monitoring, proposing that collusion may stem from imperfect exploration rather than sophisticated punishment. [Meylahn and den Boer \(2022\)](#) prove that collusion can emerge through gradient-based algorithms, providing the first theoretical convergence guarantees for tacit algorithmic collusion. [Aouad and den Boer \(2021\)](#) show that standard epsilon-greedy bandit algorithms enable tacit collusion in assortment games with sublinear regret. [Loots and den Boer \(2023\)](#) construct an explicit “Collude-or-Compete” pricing algorithm that converges to collusive prices under self-play by applying axiomatic bargaining theory. Their analysis demonstrates that algorithmic collusion can emerge when firms deploy identical algorithms that infer private demand information from observable price paths. [Brown and MacKay \(2023\)](#) show theoretically that simple pricing algorithms can increase price levels in Markov perfect equilibrium.

However, several studies identify conditions under which collusion does not emerge. [den Boer et al. \(2022\)](#) provide a critical examination, arguing that Q-learning collusion emerges only on timescales irrelevant to firms’ planning horizons and requires implicit coordination on algorithm choice. [Goyal et al. \(2023\)](#) prove that online gradient descent pricing algorithms converge to the unique Nash equilibrium under multinomial logit demand, suggesting that collusion is not universal across algorithm types. [Li and Mehrotra \(2025\)](#) establish that when firms use individual data-driven learning algorithms without access to competitor information, they naturally converge to the Nash equilibrium, indicating that common data is necessary for collusion. In auction settings, [Balseiro and Gur \(2019\)](#) demonstrate that adaptive pacing strategies constitute an approximate Nash equilibrium in large markets. On the regulatory front, [Hartline et al. \(2024\)](#) develop an auditing framework for pricing algorithms based on calibrated regret, providing tools to detect tacit coordination from observed deployment data. In mechanism design, [Gorokh et al. \(2019\)](#) characterize conditions under which mechanisms can be made resilient to collusion, though their focus on explicit side payments differs from tacit algorithmic coordination. Our work differs from this algorithmic pricing literature in a fundamental way. While these algorithms require extensive training to discover collusive strategies, LLMs arrive pretrained with business knowledge and pricing practices already encoded. The collusion mechanism operates through shared latent preferences rather than learned strategies.

LLM-based pricing and strategic behavior. Recent work examines LLM behavior in economic settings. [Fish et al. \(2024\)](#) provide the first evidence that LLM-based pricing agents converge to supra-competitive prices, with GPT-4 reaching collusive outcomes within 100 periods compared

to hundreds of thousands for Q-learning. [Wu et al. \(2024\)](#) corroborate this finding in Bertrand competition simulations, showing that LLMs collude within 400 rounds without explicit instructions to coordinate and form price agreements within 30 rounds when communication is permitted. [Robinson and Burden \(2025\)](#) find that contextual framing strongly affects LLM cooperation: real-world business scenarios yield 98% cooperation rates, compared with 37% for abstract framings. This suggests LLMs deployed for actual pricing may naturally reach collusive outcomes. [Chen et al. \(2025\)](#) show that LLMs exhibit human-like behavioral biases in operations management decisions, including framing effects and probability weighting. Our paper provides the first theoretical framework explaining why LLM-based pricing leads to collusion, identifying two mechanisms: shared latent preferences from concentrated LLM markets, and data aggregation during retraining that creates self-reinforcing feedback loops driving prices upward.

Algorithmic monoculture and shared infrastructure. [Kleinberg and Raghavan \(2021\)](#) formalize algorithmic monoculture risks, showing that widespread adoption of identical algorithms can reduce decision quality by causing all sellers to miss the same opportunities. [Bommasani et al. \(2022\)](#) demonstrate that sharing model components leads to outcome homogenization: individuals rejected by one decision-maker face rejection everywhere, creating systemic exclusion. [Black et al. \(2022\)](#) show that model multiplicity, the existence of equally accurate models with different predictions, naturally provides diversity across decision-makers, but monoculture eliminates this protective heterogeneity. Our work shows that monoculture in LLM-based pricing creates acute collusion risks. The shared latent preference in our model captures how common pretraining and concentrated LLM markets create correlated recommendations across independent sellers. Unlike traditional monoculture concerns about decision quality, we demonstrate that monoculture directly enables supra-competitive outcomes. LLM retraining with shared data further amplifies collusive tendencies over time.

3. Model

The pricing game. Following [Banchio and Mantegazza \(2022\)](#), we consider a symmetric duopoly pricing game in which two identical sellers compete by simultaneously choosing prices for their horizontally differentiated products over an infinite horizon. In each round, each seller can select either a high-price strategy (H) or a low-price strategy (L), with payoffs determined by the payoff matrix in Table 1, where $r \in (1, 2)$ denotes the relative profitability of the high-price strategy. Specifically, a higher value of r indicates that the high-price decision becomes more attractive.

LLM-based decision making. Both sellers delegate their pricing decisions to the same LLM by requesting pricing recommendations. We assume that sellers adopt these recommendations

		Seller 2	
		<i>H</i>	<i>L</i>
Seller 1	<i>H</i>	(2 <i>r</i> , 2 <i>r</i>)	(<i>r</i> , 2 + <i>r</i>)
	<i>L</i>	(2 + <i>r</i> , <i>r</i>)	(2, 2)

Table 1 Profit structure of the duopolistic price competition, where $1 < r < 2$. *H* represents the high-price strategy, while *L* indicates the low-price strategy. Adapted from Banchio and Mantegazza (2022).

rather than merely soliciting them. This assumption reflects the operational reality of algorithmic decision-making: research on algorithm appreciation demonstrates that decision-makers systematically adhere to algorithmic advice, often preferring it over human judgment (Logg et al. 2019). Once sellers delegate pricing to an AI system, manual override becomes costly. Such interventions require dedicated analyst time, disrupt automated workflows, and introduce inconsistency that complicates performance attribution. Moreover, the value proposition of LLM-based pricing lies in enabling rapid, scalable, data-driven decisions. This advantage erodes when human judgment routinely second-guesses each recommendation.

While we assume full adoption for expositional clarity, this assumption is without loss of generality. If sellers instead adopt recommendations with some probability less than 1, this partial adherence introduces additional randomness that reduces the effective correlation between the LLM’s internal preferences and the sellers’ final adopted pricing decisions. Our framework fully captures this case via the output-fidelity parameter defined below, although this parameter must be interpreted more broadly than its nominal meaning.

The LLM’s pricing behavior is characterized by two fundamental parameters: the *propensity parameter* $\theta \in [0, 1]$ and the *output fidelity* $\rho \in [0.5, 1]$. The former parameter θ represents the proportion of the LLM’s internal decision policy that allocates high-price recommendations. Formally, the LLM maintains a latent preference state unobservable to sellers, operating in either a high-price mode (denoted *H*-mode) or a low-price mode (denoted *L*-mode). This parameter embodies the LLM’s structural tendency toward certain pricing strategies, reflecting the aggregate influence of its training corpus, model architecture, and alignment procedures. Because both sellers query the same LLM, this latent preference is shared between sellers, creating an endogenous correlation in their pricing recommendations. The propensity parameter θ remains fixed until the LLM undergoes retraining, at which point it will be updated based on observed performance outcomes from seller interactions.

When $\theta > 1/2$, the *H*-mode is more likely, so the LLM tends toward high-price recommendations. Conversely, when $\theta < 1/2$, the *L*-mode predominates and low prices are favored. At the symmetric point $\theta = 1/2$, the model is equally likely to operate in either mode, representing maximal

uncertainty in its pricing preference.

The output fidelity ρ captures the alignment probability between the LLM's latent preference and its generated output. Due to stochastic generation mechanisms (e.g., sampling temperature and top- k /top- p filtering), the LLM does not deterministically produce recommendations that perfectly align with its latent preference. Specifically, conditional on adopting the H -mode, the LLM recommends strategy H to each seller with probability ρ and strategy L with probability $1 - \rho$. Conversely, conditional on the L -mode, the LLM recommends L with probability ρ and H with probability $1 - \rho$. It is worth noting that these output realizations are conditionally independent across the two sellers, given the shared latent preference, introducing idiosyncratic noise into each seller's recommendation.

When $\rho \rightarrow 1$, the shared latent preference dominates, inducing strong positive correlation in seller strategies. In contrast, when $\rho \rightarrow 0.5$, independent output noise overwhelms the preference signal, rendering strategies increasingly randomized despite the shared underlying model with a common propensity parameter θ .

This formulation also accommodates partial seller adherence, as previewed above. If a seller overrides the LLM recommendation with some probability, independently choosing a pricing strategy, this additional randomness reduces the effective alignment between the model's latent preference and the seller's realized action. Formally, partial adherence is equivalent to lowering the effective value of ρ . The output fidelity parameter thus captures both the LLM's generation stochasticity and the degree of seller adherence, with higher adherence corresponding to higher effective ρ .

Given the parameters (θ, ρ) , we can then derive the probability distribution over strategy profiles. Let p_{ij} denote the probability that Seller 1 chooses strategy i and Seller 2 chooses strategy j , where $i, j \in \{H, L\}$. The joint probabilities are:

$$p_{HH}(\theta) = \theta\rho^2 + (1 - \theta)(1 - \rho)^2, \quad (1)$$

$$p_{HL}(\theta) = p_{LH}(\theta) = \rho(1 - \rho), \quad (2)$$

$$p_{LL}(\theta) = \theta(1 - \rho)^2 + (1 - \theta)\rho^2. \quad (3)$$

Equation (1) decomposes as follows: $\theta\rho^2$ represents the probability that the model favors high prices and both outputs align with this preference, while $(1 - \theta)(1 - \rho)^2$ captures cases where the model favors low prices but both outputs deviate, yielding H for both sellers. Similar interpretations apply to (2) and (3).

Preference update mechanism. The LLM updates its propensity parameter θ through periodic retraining on seller interactions. Specifically, the LLM adjusts its pricing propensity based on

the relative performance of high-price versus low-price recommendations. Intuitively, if high-price recommendations yield higher average payoffs than low-price recommendations, the LLM should increase its propensity toward high prices, and vice versa.

This update mechanism requires the LLM to observe both sellers' pricing actions and realized payoffs. Such observability arises naturally from the data sharing policies documented in the introduction: when both sellers query the same LLM provider and share their interaction data (including adopted prices and realized profits), the provider aggregates this feedback during model retraining. As noted earlier, major providers collect user interaction data by default. Even in the absence of explicit profit reports, payoff-relevant signals emerge through behavioral patterns: continued adoption of recommendations indicates success, while abandonment or override suggests poor outcomes. Moreover, in many retail markets, pricing actions are publicly observable through price comparison platforms and web scraping. This observability parallels standard assumptions in the algorithmic collusion literature (see, e.g., Banchio and Mantegazza 2022, Calvano et al. 2020).

To formalize this intuition, we consider a batch learning framework in which the LLM is retrained after observing every batch of $b \geq 1$ decision rounds. At each retraining step, the LLM evaluates the relative performance of strategies H and L from the observed data and updates its propensity accordingly. We then consider an update rule that correctly tracks the conditional payoff difference between strategies, accounting for the dependence of strategy frequencies on the current propensity.

Let $S \in \{H, L\}$ denote a randomly sampled seller's action and Π denote the seller's realized profit in a given round. Define the *conditional payoff difference*

$$\Delta(\theta) = \mathbb{E}[\Pi | S = H, \theta] - \mathbb{E}[\Pi | S = L, \theta], \quad (4)$$

which measures the expected payoff advantage of the high-price strategy over the low-price strategy, conditional on being recommended. The sign of $\Delta(\theta)$ determines which strategy yields higher expected returns under the current propensity. A natural learning objective is for the LLM to increase θ when $\Delta(\theta) > 0$ (the high price outperforms) and decrease θ when $\Delta(\theta) < 0$ (the low price outperforms). However, since $\Delta(\theta)$ is not directly observable, the LLM must estimate it from finite samples of interaction data.

Estimating $\Delta(\theta)$ from sellers' feedback. To update its propensity, the LLM must estimate the conditional payoff difference $\Delta(\theta)$ from observed interaction data. A fundamental challenge arises: the model observes payoffs only for strategies actually recommended and adopted, not the counterfactual outcomes under alternative recommendations. To capture this selection structure, we model the estimation procedure using inverse probability weighting (IPW), a classical technique

from causal inference that corrects for selection bias by reweighting observations according to their sampling probabilities. We emphasize that our theoretical framework extends beyond this particular specification: the critical requirement is that the estimator be unbiased with bounded variance. Any estimation procedure satisfying these mild conditions will asymptotically track the same underlying performance measure, as formally established in our subsequent analysis. In particular, IPW serves as a canonical representative within this broader class, enabling a clean characterization of the LLM's learning dynamics while connecting naturally to the established literature on policy evaluation (see, e.g., Horvitz and Thompson 1952, Imbens and Rubin 2015).

Consider a single round of interaction producing actions (S_1, S_2) and payoffs (Π_1, Π_2) for the two sellers. For each seller $i \in \{1, 2\}$ we observe the pair $(S, \Pi) = (S_i, \Pi_i)$. Let

$$p_H(\theta) \triangleq \mathbb{P}(S = H \mid \theta) = \theta\rho + (1 - \theta)(1 - \rho)$$

denote the marginal probability that a seller receives recommendation H when the propensity is θ , and let $p_L(\theta) = 1 - p_H(\theta)$. The key observation is that the observed strategy S is drawn from a known distribution that depends on θ , enabling inverse probability weighting. In particular, we define the estimator

$$D(\theta) = \frac{\Pi}{p_H(\theta)} \mathbb{1}\{S = H\} - \frac{\Pi}{p_L(\theta)} \mathbb{1}\{S = L\}. \quad (5)$$

This construction provides an unbiased estimate of the conditional payoff difference from a single observation.

LEMMA 1 (UNBIASED ESTIMATION). *For any fixed $\theta \in [0, 1]$ with $p_H(\theta), p_L(\theta) \in (0, 1)$, the random variable $D(\theta)$ defined in (5) satisfies*

$$\mathbb{E}[D(\theta) \mid \theta] = \Delta(\theta).$$

Moreover, for fixed $\rho \in (1/2, 1)$, $D(\theta)$ is uniformly bounded over $\theta \in [0, 1]$.

A principled learning rule. Given the unbiased estimator, we now derive an update rule for the LLM's propensity. At the n th retraining step, the LLM observes a batch of b rounds of sellers' feedback. In particular, for each round $\ell \in \{1, \dots, b\}$ and seller $i \in \{1, 2\}$, we observe $(S_i^{(\ell)}, \Pi_i^{(\ell)})$ and compute $D_i^{(\ell)}(\theta_n)$ via (5). The batch-average estimator is

$$\bar{D}_n^{(b)} = \frac{1}{2b} \sum_{\ell=1}^b \sum_{i=1}^2 D_i^{(\ell)}(\theta_n). \quad (6)$$

This batch average remains an unbiased estimator $\mathbb{E}[\bar{D}_n^{(b)} \mid \theta_n] = \Delta(\theta_n)$.

A standard and theoretically grounded way to update a Bernoulli propensity is to update the *log-odds*. In the learning literature (see, e.g., [Cesa-Bianchi and Lugosi 2006](#)), it is equivalent to applying exponential weights or mirror descent on the two-action simplex. Specifically, let

$$z_n \triangleq \log\left(\frac{\theta_n}{1-\theta_n}\right) \in \mathbb{R}, \quad \theta_n = \sigma(z_n) \triangleq \frac{1}{1+e^{-z_n}}.$$

Given step sizes $(\gamma_n)_{n \geq 0}$ with $\gamma_n > 0$, $\sum_{n=0}^{\infty} \gamma_n = \infty$, and $\sum_{n=0}^{\infty} \gamma_n^2 < \infty$ (for example, $\gamma_n = \eta/(n+1)^\alpha$ with $\alpha \in (1/2, 1]$ and $\eta \in (0, 1]$), the LLM's propensity evolves according to

$$z_{n+1} = z_n + \gamma_n \bar{D}_n^{(b)}, \quad \theta_{n+1} = \sigma(z_{n+1}). \quad (7)$$

This update rule employs batch computations for iterative parameter refinement, naturally aligning with the stochastic gradient descent procedures used in LLM training. Moreover, it admits an intuitive interpretation. We note that

$$\theta_{n+1} - \theta_n = \sigma(z_n + \gamma_n \bar{D}_n^{(b)}) - \sigma(z_n) = \sigma'(z_n) \gamma_n \bar{D}_n^{(b)} + O(\gamma_n^2),$$

and $\sigma'(z) = \sigma(z)(1 - \sigma(z)) = \theta_n(1 - \theta_n)$. Hence,

$$\theta_{n+1} = \theta_n + \gamma_n \theta_n(1 - \theta_n) \bar{D}_n^{(b)} + O(\gamma_n^2). \quad (8)$$

Equation (8) is the first-order approximation of the log-odds update and corresponds to a two-action replicator step in evolutionary game theory, or a natural-gradient step from the perspective of information geometry. Intuitively, the LLM adjusts its propensity in the direction indicated by the payoff difference estimator. The scaling factor $\theta_n(1 - \theta_n)$ ensures that updates are larger when the propensity is intermediate and the uncertainty about which strategy is better is high, and updates are smaller near the boundaries $\theta = 0$ or $\theta = 1$, where the LLM already has strong beliefs.

4. Analysis

We analyze the long-run behavior of the LLM's propensity to make pricing recommendations under the update rule (7). In particular, we first study the large-batch regime ($b \rightarrow \infty$), in which stochastic noise vanishes. We then consider the finite-batch case using stochastic approximation, and analyze the effect of batch size. Before proceeding, we first note that the stochastic recursion (7) admits a deterministic characterization in terms of an associated ordinary differential equation (ODE). The following lemma, which adapts classical results from stochastic approximation theory ([Borkar 2008](#), [Benaïm 1999](#)), formalizes this connection.

LEMMA 2 (ODE TRACKING). *Consider the stochastic recursion (7) and let $(\mathcal{H}_n)_{n \geq 0}$ denote the natural filtration generated by the sequence (z_0, z_1, \dots, z_n) . Suppose the following conditions hold:*

(A1) step-size conditions: *The learning rates satisfy $\gamma_n > 0$ for all n , $\sum_{n=0}^{\infty} \gamma_n = \infty$, and $\sum_{n=0}^{\infty} \gamma_n^2 < \infty$.*

(A2) unbiased gradient estimation: *The batch-average estimator satisfies $\mathbb{E}[\bar{D}_n^{(b)} | \mathcal{H}_n] = \Delta(\theta_n)$.*

(A3) bounded second moments: *For any fixed $\rho \in (1/2, 1)$, there exists a constant $C < \infty$ such that $\mathbb{E}[(\bar{D}_n^{(b)})^2] \leq C$ for all n .*

Then we have

(i) (Asymptotic Tracking) *Trajectory (z_0, z_1, \dots, z_n) asymptotically tracks the solution to the mean-field ODE*

$$\dot{z}(t) = \Delta(\sigma(z(t))). \quad (9)$$

Formally, define the continuous-time interpolation $\bar{z} : [0, \infty) \rightarrow \mathbb{R}$ by setting $t_0 = 0$, $t_n = \sum_{k=0}^{n-1} \gamma_k$ for $n \geq 1$, and letting $\bar{z}(t)$ be the piecewise-linear function satisfying $\bar{z}(t_n) = z_n$. For any initial condition $z \in \mathbb{R}$, let $\Phi_t(z)$ denote the solution to the ODE (9) at time t when starting from $z(0) = z$. Then for any $T > 0$,

$$\sup_{0 \leq t \leq T} |\bar{z}(t_n + t) - \Phi_t(z_n)| \xrightarrow{n \rightarrow \infty} 0 \quad \text{almost surely.}$$

(ii) (Equilibrium Convergence) *Almost surely, every limit point of the sequence $(z_n)_{n \geq 0}$ is an equilibrium of the ODE (9), that is, a point z^* satisfying $\Delta(\sigma(z^*)) = 0$.*

Lemma 2 provides a theoretical foundation for analyzing the long-run behavior of LLM-based pricing. The result states that the noisy, discrete-time learning process (7) behaves like the smooth, deterministic dynamical system (9) over long time horizons. This ‘‘ODE method’’ reduces the analysis of a complex stochastic system to the study of a one-dimensional differential equation, whose equilibria and stability properties can be characterized explicitly. We will exploit this connection throughout our analysis.

Intuitively, condition (A1) ensures that the step sizes γ_n decay slowly enough for the algorithm to explore the parameter space (via $\sum_{n=0}^{\infty} \gamma_n = \infty$), yet fast enough for the noise to average out (via $\sum_{n=0}^{\infty} \gamma_n^2 < \infty$). Condition (A2) guarantees that the estimator $\bar{D}_n^{(b)}$ provides an unbiased signal for the true payoff advantage $\Delta(\theta_n)$, so that on average the updates point in the ‘‘correct’’ direction. Condition (A3) bounds the estimation variance, preventing the noise from overwhelming the signal. Under these conditions, the cumulative effect of the martingale noise terms vanishes in the limit, leaving only the deterministic drift $\Delta(\theta)$. The sequence $(z_n)_{n \geq 0}$ thus tracks the integral curves of the ODE, and its limit points must satisfy the equilibrium condition $\Delta(\sigma(z^*)) = 0$.

We next provide an equivalent formulation of (9) in propensity space. Specifically, applying the chain rule to the transformation $\theta(t) = \sigma(z(t))$, where $\sigma'(z) = \sigma(z)(1 - \sigma(z))$, yields an equivalent ODE

$$\dot{\theta}(t) = \theta(t)(1 - \theta(t))\Delta(\theta(t)). \quad (10)$$

This characterization will prove convenient for characterizing equilibria and their stability properties. Intuitively, the factor $\theta(1 - \theta)$ ensures that the boundaries $\theta \in \{0, 1\}$ are absorbing, while the sign of $\Delta(\theta)$ determines whether the propensity drifts toward high-price or low-price recommendations.

We characterize the equilibrium structure of the dynamical system (10) by first analyzing the asymptotic regime where the batch size $b \rightarrow \infty$. This limiting case provides analytical tractability while capturing the essential equilibrium dynamics.

4.1. Large-Batch Regime

When batch size b grows large, the law of large numbers implies that the batch-averaged estimator $\bar{D}_n^{(b)}$ concentrates around its expectation $\Delta(\theta_n)$. As $b \rightarrow \infty$, the stochastic recursion (7) converges almost surely to a deterministic recursion that tracks the ODE (10)

$$z_{n+1} = z_n + \gamma_n \Delta(\theta_n), \quad \theta_n = \sigma(z_n). \quad (11)$$

Consequently, the LLM increases its internal preference to a high-price strategy almost surely when $\Delta(\theta_n) > 0$, that is, for all $\theta_n = \theta$ such that

$$\frac{p_{HH}(\theta) \cdot 2r + p_{HL}(\theta) \cdot r}{p_{HH}(\theta) + p_{HL}(\theta)} > \frac{p_{LH}(\theta) \cdot (r+2) + p_{LL}(\theta) \cdot 2}{p_{LH}(\theta) + p_{LL}(\theta)}.$$

The left-hand side represents the expected profit conditional on receiving recommendation H , while the right-hand side is the expected profit conditional on recommendation L . The following proposition characterizes the region in (θ, ρ) space where this inequality holds.

PROPOSITION 1 (CONDITIONS FOR PRICE PROPENSITY DRIFT). *Let $r \in (1, 2)$ and $\rho \in (1/2, 1]$.*

Define

$$s(\rho, r) \triangleq \frac{2(2-r)\rho(1-\rho)}{(r-1)(2\rho-1)^2}, \quad (12)$$

and when $s(\rho, r) \leq 1$ define

$$\theta_{\pm}(\rho, r) \triangleq \frac{1}{2} \pm \frac{1}{2} \sqrt{1 - s(\rho, r)}. \quad (13)$$

Then

- (i) *If $s(\rho, r) > 1$, then $\Delta(\theta) < 0$ for all $\theta \in (0, 1)$.*

(ii) If $s(\rho, r) = 1$, then $\Delta(\theta) = 0$ if and only if $\theta = 1/2$, and $\Delta(\theta) < 0$ for all $\theta \in (0, 1) \setminus \{1/2\}$.
 (iii) If $s(\rho, r) < 1$, then $\Delta(\theta) > 0$ if and only if $\theta \in (\theta_-(\rho, r), \theta_+(\rho, r))$, with $\Delta(\theta_\pm) = 0$ and $\Delta(\theta) < 0$ outside $[\theta_-, \theta_+]$.

Proposition 1 characterizes when the learning dynamics almost surely push the LLM’s propensity θ upward, toward more frequent high-price recommendations. The sign of the conditional payoff difference $\Delta(\theta)$ governs this direction: when $\Delta(\theta) > 0$, the high-price recommendation H yields higher expected profit conditional on being played, reinforcing the LLM’s preference for H . The proposition partitions the parameter space into regions determined by the statistic $s(\rho, r)$, which captures the ratio of two competing forces. In particular, the numerator in (12) represents the cost of recommendation deviations. When one seller receives H and the other receives L , the low-price seller earns $2 + r$ while the high-price seller earns only $2r$, leading to a gap of $2 - r$ favoring L . The factor $\rho(1 - \rho)$ is the probability of such a deviation per seller pair. On the other hand, the denominator in (12) implies the benefit of coordinated high pricing. When both sellers receive H and play (H, H) , each earns $2r$ rather than the competitive payoff of 2; the per-seller gain is $2(r - 1)$. The factor $(2\rho - 1)^2$ measures the correlation strength in recommendations induced by the shared latent mode. When $s(\rho, r) < 1$, the coordination benefit dominates the deviation cost, creating a parameter region where high-price recommendations are self-reinforcing.

For any fixed $r \in (1, 2)$, the statistic $s(\rho, r)$ is strictly decreasing in ρ over $(1/2, 1)$: it diverges to $+\infty$ as $\rho \rightarrow 1/2^+$ and vanishes as $\rho \rightarrow 1$. This monotonicity reflects a fundamental tradeoff: higher fidelity simultaneously reduces miscoordinations (i.e., $\rho(1 - \rho)$ decreases) and strengthens coordination (i.e., $(2\rho - 1)^2$ increases). Consequently, for any profitability parameter $r \in (1, 2)$, there exists a critical threshold $\rho_c(r) \in (1/2, 1)$ above which $s(\rho, r) < 1$ and an upward-drift region for price propensity emerges. Therefore, sufficiently high output fidelity always enables the possibility of collusive dynamics.

We also note that even when $s(\rho, r) < 1$, the region where $\Delta(\theta) > 0$ is an interval (θ_-, θ_+) bounded away from both 0 and 1. The intuition is that at extreme propensities, the uncommon recommendation almost always signals a deviation from the recommendation to the opponent, and deviations always favor the low-price seller. Specifically, when θ is near zero and propensity strongly favors L , the latent mode is almost always L . A seller who nonetheless receives H is likely an outlier, while the opponent almost surely receives L . The resulting (H, L) outcome punishes the H -playing outlier, who earns only r compared to the opponent’s $2 + r$. Hence $\mathbb{E}[\Pi | S = H] \approx r < 2 \approx \mathbb{E}[\Pi | S = L]$, and learning drives θ further toward zero. In contrast, when θ is near one and propensity strongly favors H , the mode is almost always H . A seller who receives L is the rare outlier, likely

facing an opponent who receives H . The (L, H) outcome rewards this outlier with $2 + r$, exceeding the (H, H) payoff of $2r$ (since $r < 2$). Hence $\mathbb{E}[\Pi | S = L] \approx 2 + r > 2r \approx \mathbb{E}[\Pi | S = H]$, and learning pushes θ back down. These asymmetric outcomes drive $\Delta(\theta) < 0$ at both extremes: near $\theta = 0$ the rare H -recommendation is punished, while near $\theta = 1$ the rare L -recommendation is rewarded, but this makes L preferable to H . This creates a *basin of attraction* (defined as the region of those starting points that converge to a particular equilibrium) around the fixed point θ_+ when it exists, while preserving $\theta = 0$ as a competing attractor.

PROPOSITION 2 (COLLUSIVE BEHAVIOR IN THE LARGE-BATCH LIMIT). *Fix $r \in (1, 2)$, $\rho \in (1/2, 1]$, a step-size exponent $\alpha \in (1/2, 1]$, and a scaling constant $\eta \in (0, 1]$. Consider the step sizes $\gamma_n = \frac{\eta}{(n+1)^\alpha}$, so that $\sum_{n=0}^{\infty} \gamma_n = \infty$ and $\sum_{n=0}^{\infty} \gamma_n^2 < \infty$. Let $(\theta_n^{(b)})_{n \geq 0}$ denote the sequence generated by the stochastic recursion (7) with batch size b and initial condition $\theta_0 \in (0, 1)$. Define the critical output-fidelity threshold*

$$\rho_c(r) \triangleq \frac{1 + \sqrt{(2 - r)/r}}{2}. \quad (14)$$

If $\rho \in (1/2, 1)$, then for any fixed $N < \infty$, as $b \rightarrow \infty$ we have

$$\max_{0 \leq n \leq N} |\theta_n^{(b)} - \theta_n| \xrightarrow{\text{a.s.}} 0,$$

where $(\theta_n)_{n \geq 0}$ is the solution of the limiting recursion (11) with the same initial condition. Moreover, as $n \rightarrow \infty$, the limiting recursion satisfies:

- (i) (Low-fidelity regime) *If $\rho \in (1/2, \rho_c(r))$, then $\theta_n \rightarrow 0$ for all $\theta_0 \in (0, 1)$.*
- (ii) (Critical regime) *If $\rho = \rho_c(r)$, then $\theta_n \rightarrow 0$ for $\theta_0 \in (0, 1/2)$, and $\theta_n \rightarrow 1/2$ for $\theta_0 \in [1/2, 1)$.*
- (iii) (High-fidelity regime) *If $\rho \in (\rho_c(r), 1)$, then:*
 - (a) $\theta_n \rightarrow 0$ *if $\theta_0 \in (0, \theta_-(\rho, r))$;*
 - (b) $\theta_n \rightarrow \theta_+(\rho, r) \in (1/2, 1)$ *if $\theta_0 \in (\theta_-(\rho, r), 1)$.*
- (iv) (Perfect-fidelity regime) *If $\rho = 1$, then $\theta_n \rightarrow 1$ for all $\theta_0 \in (0, 1)$.*

Proposition 2 characterizes the long-run behavior of LLM-based pricing when retraining occurs over sufficiently large batches of interaction data. The analysis builds on Lemma 2: as $b \rightarrow \infty$, the stochastic recursion converges to its deterministic limit, and the ODE tracking result ensures that long-run outcomes correspond to equilibria of the mean-field ODE. In this regime, estimation noise becomes negligible, and the learning dynamics are governed entirely by the sign of the conditional payoff difference $\Delta(\theta)$. The proposition reveals the *collusion emergence* through a phase transition in the system's long-run behavior, governed by the critical threshold $\rho_c(r)$. This threshold marks the minimum output fidelity above which a collusive equilibrium exists: when $\rho > \rho_c(r)$, the learning

dynamics can sustain elevated prices in the long run, whereas when $\rho < \rho_c(r)$, the unique long-run outcome is competitive pricing.

Specifically, in the *low-fidelity regime* ($\rho < \rho_c(r)$), the LLM's recommendations are sufficiently noisy that miscoordination events where one seller prices high and the other prices low occur frequently. Because the low-price seller captures the market in such events, the expected payoff conditional on recommending H falls below that of recommending L . The learning dynamics, therefore, push the propensity θ toward zero, regardless of the initial condition. In the long run, the LLM learns to recommend competitive (low) prices.

In the *critical regime* ($\rho = \rho_c(r)$), the coordination benefit of mutual high pricing exactly balances the deviation cost. The equilibrium $\theta = 1/2$ exhibits one-sided stability: initial conditions $\theta_0 \geq 1/2$ converge to the symmetric equilibrium of $\theta = 1/2$, while initial conditions $\theta_0 < 1/2$ drift toward competitive pricing.

In the *high-fidelity regime* ($\rho_c(r) < \rho < 1$), the shared latent preference enables collusion when θ is sufficiently high. Specifically, when θ exceeds the threshold $\theta_-(\rho, r)$, the LLM frequently operates in H -mode. In this mode, both sellers receive the high-price recommendation with probability ρ , creating positive correlation in their pricing decisions. The resulting (H, H) outcomes yield the collusive payoff $2r$ per seller, which exceeds the competitive payoff of 2. This coordination benefit outweighs the cost of occasional miscoordination (in which one seller receives H while the other receives L), so the expected payoff conditional on receiving H exceeds that of L , and learning reinforces this elevated propensity. The system thus exhibits *bistability*: both $\theta = 0$ (competitive pricing) and $\theta = \theta_+(\rho, r)$ (collusive pricing) are locally stable, with basins of attraction separated by the unstable threshold $\theta_-(\rho, r)$. The long-run outcome depends on the initial condition: if the LLM begins with a sufficiently strong prior toward low-price recommendations ($\theta_0 < \theta_-$), it converges to competitive pricing. Otherwise, it converges to the collusive equilibrium. It is worth noting that since $\theta_+(\rho, r) < 1$, this collusive outcome emerges even though the LLM does not recommend the high price with certainty. The equilibrium is sustained because the correlation induced by the shared latent mode generates sufficiently frequent (H, H) outcomes to maintain the coordination benefit, even as occasional miscoordination events occur.

In the *perfect-fidelity regime* ($\rho = 1$), recommendations are deterministic given the latent mode. Both sellers always receive identical recommendations, eliminating miscoordination entirely. Since mutual high pricing ($2r$) always exceeds the low-pricing payoff (2), the learning dynamics drive the propensity toward full collusion ($\theta \rightarrow 1$) from any interior initial condition.

Proposition 2 provides a precise characterization of when LLM-based pricing leads to collusive outcomes. To better understand these collusive dynamics, we illustrate the proposition with the following example.

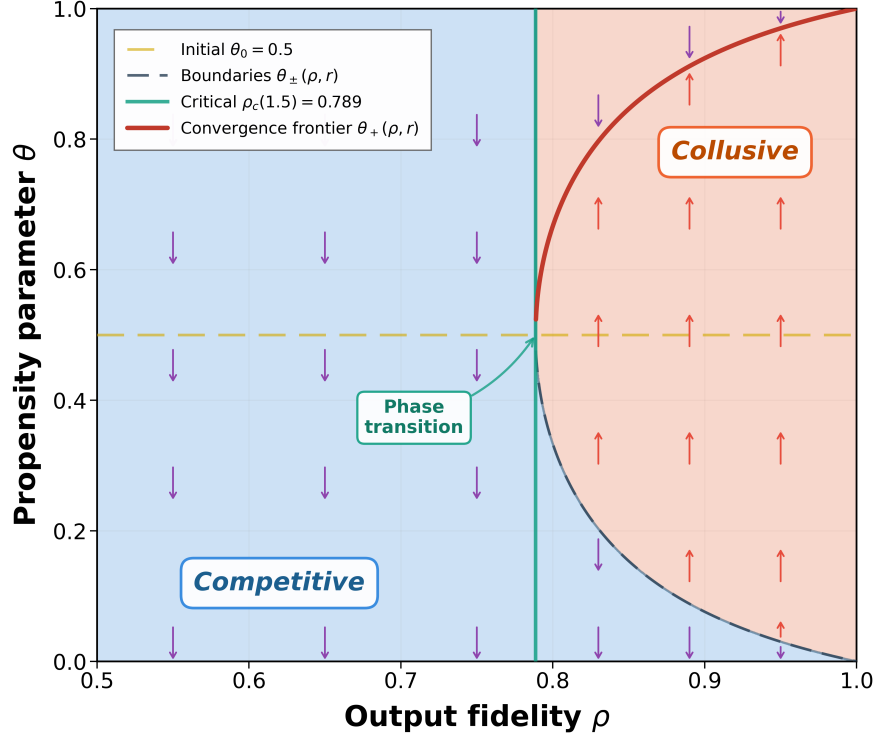


Figure 2 Phase diagram of LLM pricing dynamics in the large batch limit ($b \rightarrow \infty$) for $r = 1.5$. The shaded regions represent basins of attraction: the blue region is the competitive basin where the propensity converges to $\theta = 0$, while the pink region is the collusive basin where the propensity converges to the stable equilibrium $\theta_+(\rho, r)$. The solid red curve shows the convergence frontier $\theta_+(\rho, r)$, the long-run collusive equilibrium for each $\rho \geq \rho_c(r)$. The dashed gray curves mark the boundaries $\theta_{\pm}(\rho, r)$: the lower boundary θ_- separates the two basins, while the region between θ_- and θ_+ is where $\Delta(\theta) > 0$ (high-price strategy H outperforms L). The vertical line indicates the critical threshold $\rho_c(1.5) \approx 0.789$, separating the competitive regime (left) from the bistable regime (right). The horizontal dashed line shows the initial condition $\theta_0 = 1/2$. Arrows indicate the direction of propensity evolution: red upward arrows where $\Delta(\theta) > 0$, purple downward arrows where $\Delta(\theta) < 0$.

EXAMPLE 1 (ILLUSTRATIVE VISUALIZATION OF COLLUSION DYNAMICS). We display the (ρ, θ) parameter space as stated in Proposition 1 for $r = 1.5$ and $\theta_0 = 1/2$ in Figure 2. The $\Delta(\theta) > 0$ region is bounded by the curves $\theta_-(\rho, r)$ and $\theta_+(\rho, r)$, which collapse to a single point at $\theta = 1/2$ when $\rho = \rho_c(r)$. For $\rho < \rho_c(r)$, no such region exists, the low-price strategy L strictly dominates H for all propensities $\theta \in (0, 1)$, always driving the system toward competitive pricing ($\theta \rightarrow 0$).

The convergence frontier $\theta_+(\rho, r)$ illustrates the limit dynamics. Starting from the symmetric initial condition $\theta_0 = 1/2$ (see the horizontal dashed line), the propensity evolves according to the update rule. For any $\rho \geq \rho_c(r)$, the system converges to $\theta_+(\rho, r)$, which increases monotonically with ρ and approaches 1 as $\rho \rightarrow 1$. This monotonicity implies that higher output fidelity leads to more aggressive collusive pricing in the long run.

The phase transition at $\rho_c(r)$ (see the vertical line) highlights the critical role of output fidelity. A small increase in output fidelity from just below to just above $\rho_c(r)$ transforms the long-run outcome from purely competitive pricing ($\theta \rightarrow 0$) to partial collusion ($\theta \rightarrow \theta_+(\rho, r) \geq 1/2$). This discontinuity underscores the sensitivity of collusive outcomes to seemingly minor adjustments in LLM configuration parameters such as sampling temperature or top- p filtering.

Finally, we note that perfect output fidelity maximizes the correlation between sellers' actions and thereby sustains collusion most effectively. As ρ decreases toward $\rho_c(r)$, the $\Delta(\theta) > 0$ region narrows and eventually vanishes, indicating that stochastic noise in LLM outputs disrupts coordination and undermines collusive outcomes. \square

Example 1 illustrates several key insights from Proposition 2. First, high output fidelity enables collusion. When the LLM's output fidelity exceeds the critical threshold $\rho_c(r)$, a collusive equilibrium emerges and can be selected by the learning dynamics. This finding is particularly concerning for practical applications. In high-stakes tasks such as pricing, decision-makers typically set the LLM decoding temperature to zero (or near zero) to ensure robustness and reproducibility. This contrasts sharply with creative applications, where higher temperatures are preferred to encourage diversity. Low-temperature decoding increases output fidelity ρ , thereby inadvertently facilitating collusion. Similarly, greater seller adherence to LLM recommendations corresponds to higher effective output fidelity, further amplifying collusion risk. The threshold $\rho_c(r)$ provides a quantitative benchmark: maintaining $\rho < \rho_c(r)$ through controlled randomness in recommendations would guarantee competitive long-run outcomes, but this runs counter to standard practices that prioritize decision consistency.

Second, collusion emerges even with a moderate initial propensity. In the high-fidelity regime, Proposition 2 establishes that if the LLM's initial propensity θ_0 exceeds the threshold $\theta_-(\rho, r)$, which lies below 1/2, the learning dynamics converge to the collusive equilibrium $\theta_+(\rho, r)$. This condition is likely to be satisfied in practice, where decision-makers typically prompt LLMs with real-world business contexts rather than abstract or hypothetical framings. Two factors contribute to this tendency. First, modern LLMs are pretrained on vast corpora of real-world text, including

business literature, case studies, and strategic discussions, which extensively document the profitability of coordinated pricing. This pretraining endows the model with a prior belief that high prices are advantageous when competitors behave similarly. Second, reinforcement learning from human feedback (RLHF) and other alignment procedures tune the model to produce responses that humans find helpful and reasonable, potentially reinforcing such priors if human evaluators or users favor collusive recommendations.

Recent experimental evidence corroborates this prediction. For instance, [Robinson and Burden \(2025\)](#) find that when a strategic game is presented as a “real-world” business scenario, LLM cooperation (i.e., collusion) rates approach 98%, whereas reframing the identical rules as an “imaginary-world” scenario causes these rates to plummet to 37%. Together, these observations suggest that off-the-shelf LLMs deployed for real-world pricing decisions may enter the collusive parameter range at initialization.

Third, the interior nature of the collusive equilibrium has critical implications for detection and regulation. Because $\theta_+(\rho, r) < 1$, prices are elevated on average but not perfectly coordinated: occasional low-price recommendations create plausible deniability and complicate detection methods that rely on identifying perfect price correlation. This pattern resembles tacit collusion, where supra-competitive outcomes emerge without explicit agreement or perfectly synchronized behavior, posing challenges for antitrust enforcement that traditionally requires evidence of coordination.

4.2. Finite-Batch Regime

In contrast to the large-batch limit, in which estimation noise vanishes, practical LLM retraining operates with finite batches of interaction data. This introduces stochastic fluctuations that persist throughout the learning process and can alter the system’s trajectory. The key distinction from the large-batch regime is that equilibrium *selection* becomes random. Recall from [Proposition 2](#) that in the high-fidelity regime ($\rho > \rho_c(r)$), two stable equilibria coexist: competitive pricing ($\theta = 0$) and collusive pricing ($\theta = \theta_+$). With finite batches, identical initial conditions can lead to either outcome depending on the realized training data. We now analyze this finite-batch regime by returning to the stochastic recursion [\(7\)](#).

Specifically, we define the martingale-difference noise

$$M_{n+1} \triangleq \overline{D}_n^{(b)} - \Delta(\theta_n).$$

Because the batch-average estimator $\overline{D}_n^{(b)}$ is unbiased, we have

$$\mathbb{E}[M_{n+1} \mid \theta_n] = 0.$$

With the definition of M_{n+1} , (7) becomes

$$z_{n+1} = z_n + \gamma_n (\Delta(\theta_n) + M_{n+1}), \quad \theta_n = \sigma(z_n). \quad (15)$$

For fixed $\rho \in (1/2, 1)$, Lemma 1 implies that $\bar{D}_n^{(b)}$ (and hence M_{n+1}) has bounded second moments with $\text{Var}(M_{n+1} | \theta_n) = O(1/b)$.

The recursion (15) has a systematic component $\Delta(\theta_n)$, which drives the propensity toward its long-run value, and a noise component M_{n+1} , which introduces random fluctuations around this trend. The systematic component is identical to the large-batch case analyzed in the previous section: the same stable equilibria ($\theta = 0$ in the low-fidelity regime, and both $\theta = 0$ and θ_+ in the high-fidelity regime) govern the long-run behavior. The batch size b affects only the noise variance, leaving this equilibrium structure unchanged. However, when multiple stable equilibria coexist, noise can drive the system across basin boundaries, rendering the ultimate selection among them random. Standard results from stochastic approximation theory can be applied to establish that the propensity θ_n converges almost surely to one of the stable equilibria, though which one depends on the realized noise path. The following proposition formalizes this convergence.

PROPOSITION 3 (CONVERGENCE FOR FINITE BATCH SIZE). *Fix $r \in (1, 2)$, $\rho \in (1/2, 1)$, batch size $b \geq 1$, a step-size exponent $\alpha \in (1/2, 1]$, and a scaling constant $\eta \in (0, 1]$. Let $\gamma_n = \eta/(n+1)^\alpha$ and consider the recursion (7) from any $\theta_0 \in (0, 1)$. Then θ_n converges almost surely to a (random) equilibrium of (10). Specifically:*

- (i) *If $\rho \in (1/2, \rho_c(r))$, then $\theta_n \xrightarrow{\text{a.s.}} 0$.*
- (ii) *If $\rho = \rho_c(r)$, then $\theta_n \xrightarrow{\text{a.s.}} \theta_\infty$ where $\theta_\infty \in \{0, 1/2\}$.*
- (iii) *If $\rho \in (\rho_c(r), 1)$, then $\theta_n \xrightarrow{\text{a.s.}} \theta_\infty$ where $\theta_\infty \in \{0, \theta_+(\rho, r)\}$.*

Proposition 3 establishes that finite-batch learning converges almost surely. The argument follows the ODE method for stochastic approximation: the recursion tracks the mean-field ODE, and in one dimension, the limit set must reduce to an ODE equilibrium. Standard nonconvergence results further imply that linearly unstable equilibria are selected with probability zero. In the *low-fidelity regime* ($\rho < \rho_c(r)$), the unique long-run outcome is competitive pricing ($\theta = 0$), so convergence is deterministic despite the stochastic dynamics. At the knife-edge *critical regime* ($\rho = \rho_c(r)$), the ODE admits an additional equilibrium at $\theta = 1/2$ with one-sided stability, and finite-batch learning can converge to either $\theta = 0$ or $\theta = 1/2$ depending on the realized noise path. In the *high-fidelity regime* ($\rho > \rho_c(r)$), both $\theta = 0$ and $\theta_+(\rho, r)$ are locally stable, and which equilibrium is selected depends on the realized sequence of stochastic shocks $(M_n)_{n \geq 1}$. This path dependence is the defining feature of the finite-batch regime: identical models with identical initial conditions can converge to different long-run outcomes depending on the random training data encountered during training.

REMARK 1. When $\rho = 1$, the conditional payoff difference is constant: $\Delta(\theta) = 2r - 2 > 0$ for all $\theta \in (0, 1)$, so the mean-field ODE (10) has $\theta = 1$ as its unique attracting equilibrium. Proposition 3 is stated for $\rho < 1$ because the IPW estimator (5) becomes unbounded as $\theta \rightarrow 0$ or $\theta \rightarrow 1$ when $\rho = 1$ (i.e., an “off-policy without exploration” issue). This can be addressed by mild clipping or enforced exploration, replacing $p_H(\theta)$ and $p_L(\theta)$ in (5) with $\max\{p_H(\theta), \varepsilon\}$ and $\max\{p_L(\theta), \varepsilon\}$ for a small $\varepsilon > 0$. Under such standard stabilizations, the stochastic recursion continues to track the same ODE and converges to $\theta = 1$, for $\rho = 1$ as well.

The preceding analysis shows that convergence occurs but leaves open the question of *which* equilibrium is selected in the high-fidelity regime. The following proposition characterizes this equilibrium selection and clarifies how the batch size governs the selection probability.

PROPOSITION 4 (EQUILIBRIUM SELECTION AND THE EFFECT OF BATCH SIZE). *Fix $r \in (1, 2)$ and $\rho \in (\rho_c(r), 1)$, and let $\theta_-(\rho, r) < \theta_+(\rho, r)$ denote the unstable and stable interior equilibria from Proposition 1. Fix step sizes $\gamma_n = \eta/(n+1)^\alpha$ with $\alpha \in (1/2, 1]$ and $\eta \in (0, 1]$, and consider the stochastic recursion (7) with batch size $b \geq 1$ from an initial condition $\theta_0 \in (0, 1)$. Define the collision probability*

$$p_+(b, \theta_0) \triangleq \mathbb{P}\left(\lim_{n \rightarrow \infty} \theta_n = \theta_+(\rho, r)\right).$$

Then the following holds.

(i) (FINITE-HORIZON TRACKING WITH EXPLICIT b DEPENDENCE). *For every $T > 0$ and every $\varepsilon > 0$, there exists a constant $C = C(T, \rho, r, \alpha, \eta) < \infty$, independent of b , such that*

$$\mathbb{P}\left(\sup_{0 \leq t \leq T} |\bar{\theta}(t) - \theta^{\text{det}}(t)| > \varepsilon\right) \leq \frac{C}{b\varepsilon^2},$$

where $\bar{\theta}(t) \triangleq \sigma(\bar{z}(t))$ is the continuous-time interpolation of the stochastic sequence (z_n) (as in Lemma 2) and $\theta^{\text{det}}(t)$ is the continuous-time interpolation of the deterministic (large-batch) recursion (11) started from the same θ_0 . In particular, $\sup_{0 \leq t \leq T} |\bar{\theta}(t) - \theta^{\text{det}}(t)| = O_p(1/\sqrt{b})$.

(ii) (LOCK-IN AWAY FROM THE SEPARATRIX). *Fix $\delta \in (0, 1/2)$ and define*

$$K_+(\delta) \triangleq [\theta_- + \delta, 1 - \delta], \quad K_-(\delta) \triangleq [\delta, \theta_- - \delta].$$

There exist constants $c_\delta > 0$ and $C_\delta < \infty$ such that, for all $b \geq 1$,

$$\sup_{\theta_0 \in K_+(\delta)} (1 - p_+(b, \theta_0)) \leq C_\delta e^{-c_\delta b \delta^2}, \quad \sup_{\theta_0 \in K_-(\delta)} p_+(b, \theta_0) \leq C_\delta e^{-c_\delta b \delta^2}.$$

Consequently, for any fixed $\theta_0 \neq \theta_-$ we have

$$\lim_{b \rightarrow \infty} p_+(b, \theta_0) = \mathbb{1}\{\theta_0 > \theta_-\}.$$

(iii) (TRANSITION REGION WIDTH). For every $\epsilon \in (0, 1/2)$ and every $\delta_0 \in (0, 1/2)$ with $\theta_- \in (\delta_0, 1 - \delta_0)$, there exists $K = K(\rho, r, \alpha, \eta, \epsilon, \delta_0) > 0$ such that for all $b \geq 1$ and all $\theta_0 \in [\delta_0, 1 - \delta_0]$,

$$p_+(b, \theta_0) \in (\epsilon, 1 - \epsilon) \implies |\theta_0 - \theta_-| \leq \frac{K}{\sqrt{b}}.$$

Proposition 4 makes precise that equilibrium selection in the finite-batch regime is governed by two forces: deterministic drift and batch-induced noise. Part (i) quantifies finite-horizon tracking of the large-batch recursion, with deviations scaling as $O_p(1/\sqrt{b})$. Part (ii) turns this tracking into an equilibrium selection statement: starting a fixed margin δ above (below) the unstable threshold θ_- , the probability of selecting the “wrong” equilibrium decays at rate $e^{-cb\delta^2}$. The proof of Part (ii) is a one-dimensional barrier argument: reaching the wrong basin requires the weighted noise martingale to overcome a deterministic log-odds gap of order δ . Part (iii) summarizes the implication for comparative statics: the only initial conditions that yield a nontrivial mixture of competitive and collusive outcomes lie in an $O(1/\sqrt{b})$ neighborhood of θ_- .

EXAMPLE 2 (BATCH SIZE AND COLLUSION PROBABILITY). We illustrate the effect of the batch size on equilibrium selection using the same parameter setting as Example 1: $r = 1.5$ and $\theta_0 = 1/2$. We set $\rho = 0.85$, which exceeds the critical threshold $\rho_c(1.5) \approx 0.789$. For these parameters, $\theta_- \approx 0.154$ and $\theta_+ \approx 0.846$. Since the initial propensity $\theta_0 = 1/2$ exceeds θ_- , the deterministic dynamics (i.e., the large-batch limit) would converge to the collusive equilibrium θ_+ . Following standard practice in the stochastic approximation literature, we set the step size as $\gamma_n = 1/(n+1)^\alpha$. We note that condition (A1) requires $\alpha \in (1/2, 1]$. We thus set $\alpha = 2/3$ to ensure practical convergence within the simulation horizon. Figure 3 displays 20 independent trajectories of θ_n for batch sizes $b \in \{1, 4, 16, 64\}$, along with their sample means.

Several patterns emerge. First, all trajectories across all batch sizes eventually stabilize, consistent with the almost-sure convergence established in Proposition 3. Second, the variance of the trajectories decreases markedly with the batch size. For $b = 1$, trajectories exhibit substantial volatility and frequently cross the unstable threshold θ_- . For $b = 64$, trajectories remain tightly concentrated around the mean path and converge to the theoretical equilibrium $\theta_+ \approx 0.846$. Third, the fraction of trajectories converging to the collusive equilibrium θ_+ increases with the batch size in this simulation: 15% for $b = 1$, 70% for $b = 4$, 95% for $b = 16$, and 100% for $b = 64$. This pattern is consistent with Proposition 4, which predicts that when $\theta_0 > \theta_-$, the collusion probability rises toward one as batch noise vanishes. \square

Example 2 carries important implications for understanding collusion risk in practice. Proposition 4 implies that when the initial propensity lies above the unstable threshold θ_- , increasing

Convergence Trajectories: $\rho = 0.85, r = 1.5, \theta_0 = 0.5$

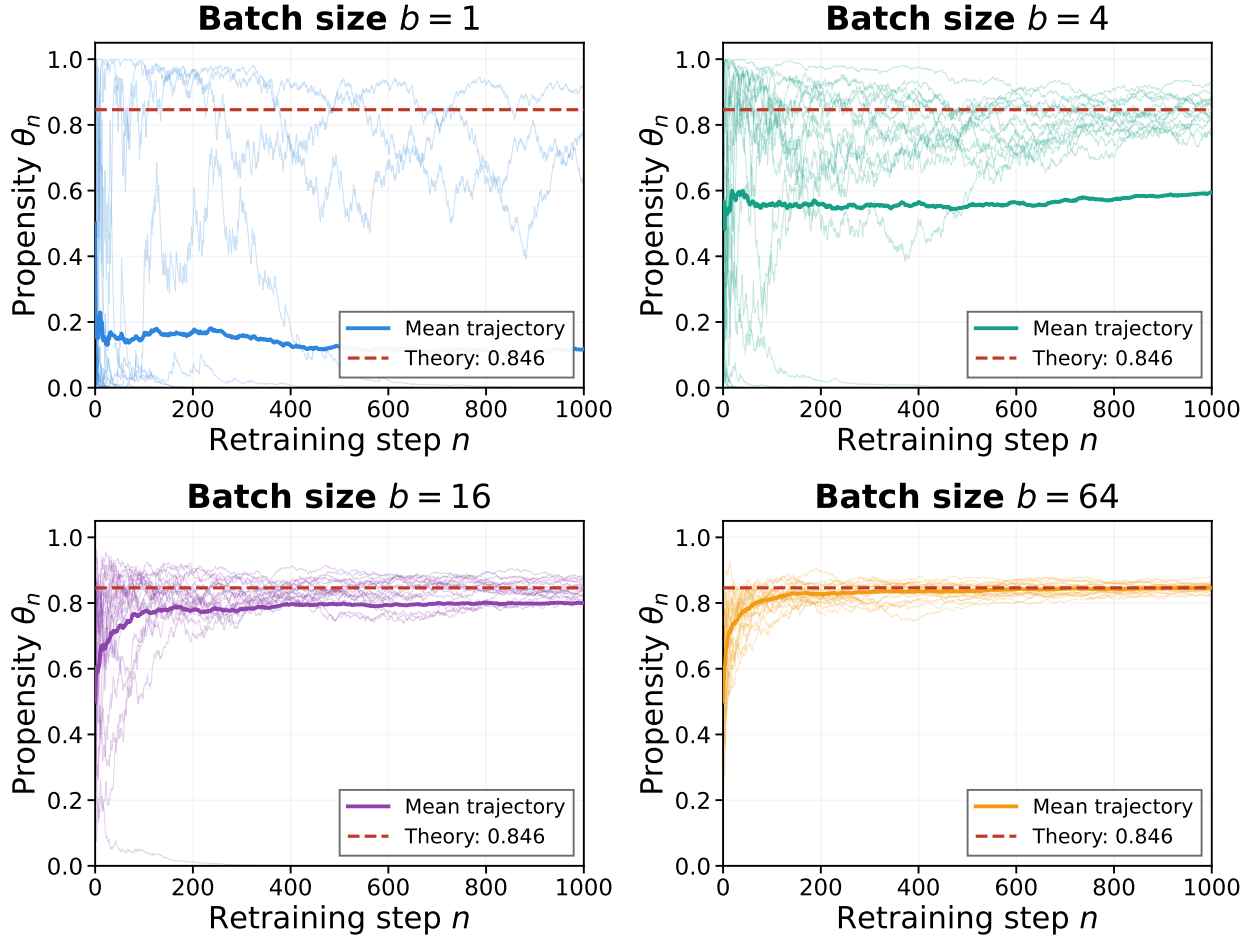


Figure 3 Convergence trajectories of propensity θ_n for different batch sizes. Each panel displays 20 independent replications (faint lines) and their sample mean (bold line) for the batch size $b \in \{1, 4, 16, 64\}$. The horizontal dashed line indicates the theoretical collusive equilibrium $\theta_+(\rho, r) \approx 0.846$. Parameters: $\rho = 0.85, r = 1.5, \theta_0 = 1/2$. Larger batch sizes reduce trajectory variance and increase the probability of converging to the collusive equilibrium.

the batch size suppresses noise and pushes the selection probability closer to the large-batch prediction of collusion. In the context of LLM-based pricing, the batch size b corresponds to the number of pricing rounds accumulated before each retraining update. In practice, retraining a large language model from scratch is prohibitively expensive, requiring months of computation on thousands of specialized accelerators. Major LLM providers therefore perform full retraining infrequently: OpenAI, Anthropic, and Google typically release major model updates every 6–12 months. Between major releases, models may receive incremental updates via parameter-efficient

fine-tuning or retrieval augmentation, but the core model weights, which encode the propensity θ in our model, remain fixed mainly. This operational reality translates directly into large effective batch sizes.

Coupled with the fact that real-world LLMs likely possess initial propensities $\theta_0 > \theta_-$ owing to pretraining on business corpora and RLHF alignment, Proposition 4 delivers a striking implication: larger retraining intervals can increase collusion risk by suppressing the noise that might otherwise push the system across the unstable threshold toward competitive pricing.

5. Conclusion

This paper develops a theoretical framework to analyze the emergence of collusion when sellers delegate pricing decisions to a large language model. Our analysis identifies a fundamental mechanism: the LLM’s shared latent preference creates correlated recommendations across sellers, and a learning process that updates the model’s propensity based on observed performance can drive prices toward collusive levels without any explicit coordination.

Our framework is subject to several limitations that suggest directions for future research. First, the model considers a duopoly setting with two sellers. Extending the analysis to N sellers introduces two opposing forces: more sellers increase the probability of at least one recommendation miscoordination, and miscoordinations favor low-price sellers, potentially undermining collusion. Simultaneously, however, the LLM creates market-wide correlation, as all N sellers receive signals drawn from the same latent preference, amplifying the monoculture effect. A central research question can be how the critical fidelity threshold ρ_c varies with N : Does market fragmentation protect against, or amplify, LLM-induced collusion?

Second, our model assumes that sellers query the LLM without historical context, so both receive recommendations drawn from the same propensity θ . In practice, queries may incorporate historical pricing data, sales outcomes, or competitor behavior. With such context, the LLM could adapt its recommendations to each seller’s history through in-context learning (Brown et al. 2020), potentially providing different policies to different sellers within each batch. One seller might receive signals that push toward collusive pricing, while another receives signals that push toward competitive pricing. When these divergent experiences are merged during retraining, the key question is whether policies converge to a common equilibrium or persistently remain heterogeneous. This connects to cutting-edge topics in machine learning, including continual learning, in which models must learn from sequential, potentially conflicting data streams (Parisi et al. 2019), and catastrophic forgetting, in which training on new data overwrites previously learned knowledge (Kirkpatrick et al. 2017). Understanding how these dynamics interact with the collusion mechanisms identified in this paper presents an important direction for future research.

References

Abada, Ibrahim, Xavier Lambin. 2023. Artificial intelligence: Can seemingly collusive outcomes be avoided? *Management Science* **69**(9) 5042–5065.

Aouad, Ali, Arnoud V den Boer. 2021. Algorithmic collusion in assortment games. *Available at SSRN 3930364* .

Assad, Stephanie, Robert Clark, Daniel Ershov, Lei Xu. 2024. Algorithmic pricing and competition: Empirical evidence from the German retail gasoline market. *Journal of Political Economy* **132**(3) 723–771.

Balseiro, Santiago R, Yonatan Gur. 2019. Learning in repeated auctions with budgets: Regret minimization and equilibrium. *Management Science* **65**(9) 3952–3968.

Banchio, Martino, Giacomo Mantegazza. 2022. Artificial intelligence and spontaneous collusion. *arXiv preprint arXiv:2202.05946* .

Benaïm, Michel. 1999. Dynamics of stochastic approximation algorithms. *Séminaire de Probabilités XXXIII* 1–68.

Bichler, Martin, Jonas Durmann, Markus Oberlechner. 2025. Algorithmic pricing and algorithmic collusion. *Business & Information Systems Engineering* **67** 971–979.

Black, Emily, Manish Raghavan, Solon Barocas. 2022. Model multiplicity: Opportunities, concerns, and solutions. *Proceedings of the 2022 ACM Conference on Fairness, Accountability, and Transparency*. 850–863.

Bommasani, Rishi, Kathleen A Creel, Ananya Kumar, Dan Jurafsky, Percy Liang. 2022. Picking on the same person: Does algorithmic monoculture lead to outcome homogenization? *Advances in Neural Information Processing Systems*, vol. 35. 3663–3678.

Borkar, Vivek S. 2008. *Stochastic Approximation: A Dynamical Systems Viewpoint*. Cambridge University Press, Cambridge, UK.

Brown, Tom, Benjamin Mann, Nick Ryder, Melanie Subbiah, Jared D Kaplan, Prafulla Dhariwal, Arvind Neelakantan, Pranav Shyam, Girish Sastry, Amanda Askell, et al. 2020. Language models are few-shot learners. *Advances in Neural Information Processing Systems*, vol. 33. 1877–1901.

Brown, Zach Y, Alexander MacKay. 2023. Competition in pricing algorithms. *American Economic Journal: Microeconomics* **15**(2) 109–156.

Calvano, Emilio, Giacomo Calzolari, Vincenzo Denicolò, Sergio Pastorello. 2020. Artificial intelligence, algorithmic pricing, and collusion. *American Economic Review* **110**(10) 3267–3297.

Cesa-Bianchi, Nicolò, Gábor Lugosi. 2006. *Prediction, Learning, and Games*. Cambridge University Press, Cambridge, UK.

Chen, Yang, Samuel Kirshner, Anton Ovchinnikov, Meena Andiappan, Tracy Jenkin. 2025. A manager and an AI walk into a bar: Does ChatGPT make biased decisions like we do? *Manufacturing & Service Operations Management* **27**(2) 354–368.

Cooper, William L, Tito Homem-de Mello, Anton J Kleywegt. 2015. Learning and pricing with models that do not explicitly incorporate competition. *Operations Research* **63**(1) 86–103.

den Boer, Arnoud V, Janusz M Meylahn, Maarten Pieter Schinkel. 2022. Artificial collusion: Examining supracompetitive pricing by Q-learning algorithms. *Tinbergen Institute Discussion Paper* .

Durrett, Rick. 2019. *Probability: Theory and Examples*. 5th ed. Cambridge University Press, Cambridge, UK.

Fish, Sara, Yannai A Gonczarowski, Ran I Shorrer. 2024. Algorithmic collusion by large language models. *arXiv preprint arXiv:2404.00806* 7.

Gorokh, Artur, Siddhartha Banerjee, Krishnamurthy Iyer. 2019. When bribes are harmless: The power and limits of collusion-resilient mechanism design. *Available at SSRN* 3125003 .

Goyal, Vineet, Shukai Li, Sanjay Mehrotra. 2023. Learning to price under competition for multinomial logit demand. *Available at SSRN* 4572453 .

Hansen, Karsten T, Kanishka Misra, Mallesh M Pai. 2021. Frontiers: Algorithmic collusion: Supra-competitive prices via independent algorithms. *Marketing Science* **40**(1) 1–12.

Hartline, Jason D, Sheng Long, Chenhao Zhang. 2024. Regulation of algorithmic collusion. *Proceedings of the 2024 Symposium on Computer Science and Law*. 98–108.

Horvitz, Daniel G, Donovan J Thompson. 1952. A generalization of sampling without replacement from a finite universe. *Journal of the American Statistical Association* **47**(260) 663–685.

Imbens, Guido W, Donald B Rubin. 2015. *Causal Inference in Statistics, Social, and Biomedical Sciences*. Cambridge University Press, Cambridge, UK.

Kirkpatrick, James, Razvan Pascanu, Neil Rabinowitz, Joel Veness, Guillaume Desjardins, Andrei A Rusu, Kieran Milan, John Quan, Tiago Ramalho, Agnieszka Grabska-Barwinska, et al. 2017. Overcoming catastrophic forgetting in neural networks. *Proceedings of the National Academy of Sciences* **114**(13) 3521–3526.

Klein, Timo. 2021. Autonomous algorithmic collusion: Q-learning under sequential pricing. *RAND Journal of Economics* **52**(3) 538–558.

Kleinberg, Jon, Manish Raghavan. 2021. Algorithmic monoculture and social welfare. *Proceedings of the National Academy of Sciences* **118**(22) e2018340118.

Li, Shukai, Sanjay Mehrotra. 2025. Adaptive learning in uncertain and sequential competition. *Operations Research* .

Logg, Jennifer M, Julia A Minson, Don A Moore. 2019. Algorithm appreciation: People prefer algorithmic to human judgment. *Organizational Behavior and Human Decision Processes* **151** 90–103.

Loots, Thomas, Arnoud V den Boer. 2023. Data-driven collusion and competition in a pricing duopoly with multinomial logit demand. *Production and Operations Management* **32**(4) 1169–1186.

Meylahn, Janusz M, Arnoud V den Boer. 2022. Learning to collude in a pricing duopoly. *Manufacturing & Service Operations Management* **24**(5) 2577–2594.

Parisi, German I, Ronald Kemker, Jose L Part, Christopher Kanan, Stefan Wermter. 2019. Continual lifelong learning with neural networks: A review. *Neural Networks* **113** 54–71.

Robinson, Isaac, John Burden. 2025. Framing the game: How context shapes LLM decision-making. *arXiv preprint arXiv:2503.04840* .

Wang, Hairu, Sheng You, Qiheng Zhang, Xike Xie, Shuguang Han, Yuchen Wu, Fei Huang, Jufeng Chen. 2025. LLP: LLM-based product pricing in e-commerce. *arXiv preprint arXiv:2510.09347* .

Wu, Zengqing, Run Peng, Shuyuan Zheng, Qianying Liu, Xu Han, Brian I Kwon, Makoto Onizuka, Shaojie Tang, Chuan Xiao. 2024. Shall we team up: Exploring spontaneous cooperation of competing LLM agents. *Findings of the Association for Computational Linguistics: EMNLP 2024*. 5163–5186.

Online Appendix to “LLM Collusion”: Supplementary Derivations and Proofs

A. Proofs

Proof of Lemma 1. For fixed θ , by the law of total expectation,

$$\begin{aligned}\mathbb{E}[D(\theta) | \theta] &= \frac{1}{p_H(\theta)} \mathbb{E}[\Pi \mathbb{1}\{S = H\}] - \frac{1}{p_L(\theta)} \mathbb{E}[\Pi \mathbb{1}\{S = L\}] \\ &= \frac{\mathbb{P}(S = H)}{p_H(\theta)} \mathbb{E}[\Pi | S = H] - \frac{\mathbb{P}(S = L)}{p_L(\theta)} \mathbb{E}[\Pi | S = L] \\ &= \mathbb{E}[\Pi | S = H] - \mathbb{E}[\Pi | S = L] = \Delta(\theta).\end{aligned}$$

For the boundedness claim, note that payoffs are bounded and, for any fixed $\rho \in (1/2, 1)$,

$$\inf_{\theta \in [0,1]} \min\{p_H(\theta), p_L(\theta)\} = 1 - \rho > 0,$$

and with $\Pi_{\max} \triangleq \max\{r, 2r, 2 + r, 2\} = 2 + r$, we have $|D(\theta)| \leq \Pi_{\max}/(1 - \rho) < \infty$ uniformly in θ . \square

Proof of Lemma 2. We organize the proof into six steps. Steps 1 to 5 establish the tracking statement in part (i) for the log-odds recursion. Step 6 works in propensity space to conclude part (ii).

Step 1: Drift-noise decomposition. Rewrite the recursion (7) as

$$z_{n+1} = z_n + \gamma_n [\Delta(\theta_n) + M_{n+1}], \quad (\text{A.1})$$

where $\theta_n = \sigma(z_n)$ and the noise term is defined as

$$M_{n+1} := \overline{D}_n^{(b)} - \Delta(\theta_n).$$

By assumption (A2), the sequence $(M_{n+1})_{n \geq 0}$ is a martingale difference sequence adapted to the filtration $(\mathcal{H}_n)_{n \geq 0}$:

$$\mathbb{E}[M_{n+1} | \mathcal{H}_n] = \mathbb{E}[\overline{D}_n^{(b)} | \mathcal{H}_n] - \Delta(\theta_n) = 0.$$

Moreover, by assumption (A3) and the boundedness of $\Delta(\cdot)$ established in Lemma 1, the second moments are uniformly bounded:

$$\sup_{n \geq 0} \mathbb{E}[M_{n+1}^2] \leq 2 \sup_n \mathbb{E}[(\overline{D}_n^{(b)})^2] + 2 \sup_{\theta \in [0,1]} |\Delta(\theta)|^2 < \infty. \quad (\text{A.2})$$

Step 2: Almost-sure convergence of the noise sum. Define the partial sums $W_n := \sum_{k=0}^{n-1} \gamma_k M_{k+1}$. We claim that $(W_n)_{n \geq 0}$ converges almost surely to a finite limit.

To see this, observe that $(W_n, \mathcal{H}_n)_{n \geq 0}$ is a martingale and

$$\mathbb{E}[W_n^2] = \sum_{k=0}^{n-1} \gamma_k^2 \mathbb{E}[M_{k+1}^2] \leq C_M \sum_{k=0}^{n-1} \gamma_k^2,$$

where $C_M := \sup_k \mathbb{E}[M_{k+1}^2] < \infty$ by (A.2). Since $\sum_{k=0}^{\infty} \gamma_k^2 < \infty$, the martingale (W_n) is L^2 -bounded. By the martingale convergence theorem (Durrett 2019, Theorem 5.4.9), W_n converges almost surely (and in L^2) to a finite limit W_{∞} .

Step 3: Regularity of the drift function. Define $h : \mathbb{R} \rightarrow \mathbb{R}$ by $h(z) := \Delta(\sigma(z))$. We verify that h is globally Lipschitz and bounded.

The sigmoid function $\sigma(z) = (1 + e^{-z})^{-1}$ is infinitely differentiable with

$$\sigma'(z) = \sigma(z)(1 - \sigma(z)) \in (0, 1/4] \quad \text{for all } z \in \mathbb{R}.$$

By construction, $\Delta(\theta)$ admits an explicit rational expression in θ , with denominator $p_H(\theta)p_L(\theta)$. For $\rho \in (1/2, 1)$, Lemma 1 shows that $p_H(\theta), p_L(\theta) \geq 1 - \rho > 0$ for all $\theta \in [0, 1]$, so Δ is continuously differentiable on $[0, 1]$ and $\sup_{\theta \in [0, 1]} |\Delta'(\theta)| < \infty$. Consequently, $h = \Delta \circ \sigma$ is continuously differentiable on \mathbb{R} and

$$|h'(z)| = |\Delta'(\sigma(z))| \sigma'(z) \leq \frac{1}{4} \sup_{\theta \in [0, 1]} |\Delta'(\theta)|,$$

which implies a global Lipschitz constant. In addition, $|h(z)| \leq \sup_{\theta \in [0, 1]} |\Delta(\theta)|$ for all z .

Step 4: Discrete-to-continuous comparison via Gronwall's inequality. Fix a horizon $T > 0$. For any initial condition $z \in \mathbb{R}$, let $\Phi_t(z)$ denote the solution to the ODE $\dot{z} = h(z)$ at time t when starting from $z(0) = z$. We compare the discrete sequence (z_n) to the ODE trajectory $(\Phi_{t-t_n}(z_n))_{t \geq t_n}$.

For $t \in [t_n, t_{n+1}]$, the ODE solution starting from z_n satisfies

$$\Phi_{t-t_n}(z_n) = z_n + \int_0^{t-t_n} h(\Phi_s(z_n)) ds.$$

In particular, setting $H := \sup_z |h(z)|$ and L to be a global Lipschitz constant for h , we have

$$|\Phi_{\gamma_n}(z_n) - z_n - \gamma_n h(z_n)| = \left| \int_0^{\gamma_n} (h(\Phi_s(z_n)) - h(z_n)) ds \right| \leq \int_0^{\gamma_n} L |\Phi_s(z_n) - z_n| ds \leq \int_0^{\gamma_n} L s H ds = \frac{LH}{2} \gamma_n^2.$$

Combining this with (A.1), the one-step error $\varepsilon_n := z_{n+1} - \Phi_{\gamma_n}(z_n)$ satisfies

$$|\varepsilon_n| \leq \gamma_n |M_{n+1}| + \frac{LH}{2} \gamma_n^2.$$

Iterating and applying a discrete Gronwall argument yields a uniform bound for the deviation between the interpolated path and the ODE trajectory over $[t_n, t_n + T]$ in terms of the martingale increments $W_m - W_n$ and the tail sum $\sum_{k=n}^{\infty} \gamma_k^2$.

Step 5: Tracking error decay. Define the tracking error over a fixed time horizon $T > 0$ as

$$V_n := \sup_{0 \leq t \leq T} |\bar{z}(t_n + t) - \Phi_t(z_n)|.$$

Let $N_T(n)$ denote the number of discrete steps in the time window $[t_n, t_n + T]$. Since h is globally Lipschitz and bounded, applying the discrete Gronwall inequality to the one-step errors from Step 4 yields a constant $C_T < \infty$ (depending only on T , L , and H) such that

$$V_n \leq C_T \left(\sup_{m \geq n} |W_m - W_n| + \sum_{k=n}^{\infty} \gamma_k^2 \right).$$

From Step 2, the partial sums $W_m := \sum_{k=0}^{m-1} \gamma_k M_{k+1}$ converge almost surely to a finite limit W_∞ . Therefore,

$$\sup_{m \geq n} |W_m - W_n| \rightarrow 0 \quad \text{a.s.}$$

as $n \rightarrow \infty$. Since $\sum_{k=0}^{\infty} \gamma_k^2 < \infty$, the tail sum also vanishes: $\sum_{k=n}^{\infty} \gamma_k^2 \rightarrow 0$. Combining these estimates yields $V_n \rightarrow 0$ almost surely, establishing part (i).

Step 6: Limit set characterization. Let z^* be a limit point of (z_n) and let $z_{n_j} \rightarrow z^*$ along a subsequence. Then $\theta_{n_j} := \sigma(z_{n_j}) \rightarrow \theta^* := \sigma(z^*)$ with $\theta^* \in (0, 1)$. We now work in propensity space.

By a second-order Taylor expansion of σ , there exists ξ_n between z_n and z_{n+1} such that

$$\theta_{n+1} = \theta_n + \gamma_n \sigma'(z_n) \bar{D}_n^{(b)} + \frac{1}{2} \sigma''(\xi_n) \gamma_n^2 (\bar{D}_n^{(b)})^2 = \theta_n + \gamma_n \theta_n (1 - \theta_n) \bar{D}_n^{(b)} + \frac{1}{2} \sigma''(\xi_n) \gamma_n^2 (\bar{D}_n^{(b)})^2.$$

Write $\bar{D}_n^{(b)} = \Delta(\theta_n) + M_{n+1}$ and define

$$F(\theta) := \theta(1 - \theta) \Delta(\theta), \quad \widetilde{M}_{n+1} := \theta_n (1 - \theta_n) M_{n+1}, \quad r_{n+1} := \frac{1}{2} \sigma''(\xi_n) \gamma_n (\bar{D}_n^{(b)})^2.$$

Then the propensity recursion becomes

$$\theta_{n+1} = \theta_n + \gamma_n (F(\theta_n) + \widetilde{M}_{n+1} + r_{n+1}).$$

Since $|\sigma''(z)| = |\sigma(z)(1 - \sigma(z))(1 - 2\sigma(z))| \leq 1/4$ for all z , we have

$$\sum_{n=0}^{\infty} \gamma_n |r_{n+1}| \leq \frac{1}{8} \sum_{n=0}^{\infty} \gamma_n^2 (\bar{D}_n^{(b)})^2 < \infty \quad \text{a.s.},$$

where the almost-sure finiteness follows from (A1) and (A3) by Fubini's theorem. Moreover, (\widetilde{M}_{n+1}) is a martingale difference sequence with uniformly bounded second moments since $\theta_n (1 - \theta_n) \leq 1/4$.

Standard stochastic approximation results imply that the piecewise-linear interpolation of (θ_n) is an asymptotic pseudotrajectory of the ODE $\dot{\theta} = F(\theta)$, which is (10). Since (θ_n) is bounded,

Benaïm (1999, Theorem 5.7) implies that its ω -limit set is internally chain transitive for this one-dimensional flow. In one dimension, any internally chain transitive set must be contained in the equilibrium set $\{\theta : F(\theta) = 0\}$. Therefore, every limit point θ^* satisfies $F(\theta^*) = 0$. For $\theta^* \in (0, 1)$ this reduces to $\Delta(\theta^*) = 0$, which is equivalent to $\Delta(\sigma(z^*)) = 0$. This establishes part (ii) and completes the proof. \square

Proof of Proposition 1. Let $S_i \in \{H, L\}$ denote the recommendation to Seller i and let Π_i denote Seller i 's profit in a single period. From Table 1:

$$\begin{aligned} (H, H) : & \quad \Pi_1 = 2r, \quad \Pi_2 = 2r, \\ (H, L) : & \quad \Pi_1 = r, \quad \Pi_2 = 2 + r, \\ (L, H) : & \quad \Pi_1 = 2 + r, \quad \Pi_2 = r, \\ (L, L) : & \quad \Pi_1 = 2, \quad \Pi_2 = 2. \end{aligned}$$

Using the joint probabilities (1)–(3), the conditional expected profits are

$$\mathbb{E}[\Pi_1 | S_1 = H, \theta] = \frac{p_{HH}(\theta) \cdot 2r + p_{HL}(\theta) \cdot r}{p_{HH}(\theta) + p_{HL}(\theta)}, \quad (\text{A.3})$$

$$\mathbb{E}[\Pi_1 | S_1 = L, \theta] = \frac{p_{LH}(\theta) \cdot (2 + r) + p_{LL}(\theta) \cdot 2}{p_{LH}(\theta) + p_{LL}(\theta)}. \quad (\text{A.4})$$

The same expressions hold for Seller 2 by symmetry. Let $A := p_{HH}(\theta)$, $B := p_{LL}(\theta)$, and $q := p_{HL}(\theta) = p_{LH}(\theta) = \rho(1 - \rho)$. The condition $\Delta(\theta) \geq 0$ is equivalent to

$$r(2A + q)(q + B) \geq (A + q)((r + 2)q + 2B), \quad (\text{A.5})$$

which follows by cross-multiplying (A.3)–(A.4).

Let $\kappa \triangleq \rho^2 - (1 - \rho)^2 = 2\rho - 1$. Then

$$A = (1 - \rho)^2 + \kappa\theta, \quad B = \rho^2 - \kappa\theta.$$

Substituting these expressions into (A.5) and simplifying yields

$$\theta(1 - \theta) \geq K(\rho, r) \triangleq \frac{(2 - r)\rho(1 - \rho)}{2(r - 1)(2\rho - 1)^2}. \quad (\text{A.6})$$

Define $s(\rho, r) \triangleq 4K(\rho, r)$, as in (12). Then (A.6) is equivalent to $\theta(1 - \theta) \geq s(\rho, r)/4$.

The function $f(\theta) = \theta(1 - \theta)$ is concave on $[0, 1]$ and attains its maximum $1/4$ at $\theta = 1/2$. Consider

$$g(\theta) \triangleq \theta^2 - \theta + \frac{s(\rho, r)}{4}.$$

Then $\theta(1 - \theta) \geq s/4$ is equivalent to $g(\theta) \leq 0$. The discriminant of g is $1 - s(\rho, r)$.

Case $s(\rho, r) > 1$. Then $1 - s < 0$ and $g(\theta) > 0$ for all θ , so (A.6) never holds and therefore $\Delta(\theta) < 0$ for all $\theta \in (0, 1)$.

Case $s(\rho, r) = 1$. Then $g(\theta) = (\theta - 1/2)^2$, so (A.6) holds if and only if $\theta = 1/2$, implying $\Delta(1/2) = 0$ and $\Delta(\theta) < 0$ for $\theta \neq 1/2$.

Case $s(\rho, r) < 1$. Then g has two real roots

$$\theta_{\pm} = \frac{1}{2} \pm \frac{1}{2} \sqrt{1 - s(\rho, r)},$$

and $g(\theta) \leq 0$ if and only if $\theta \in [\theta_-, \theta_+]$. This implies $\Delta(\theta) > 0$ for $\theta \in (\theta_-, \theta_+)$, with $\Delta(\theta_{\pm}) = 0$ and $\Delta(\theta) < 0$ outside $[\theta_-, \theta_+]$. \square

Proof of Proposition 2. The proof proceeds in three parts: (i) establishing almost-sure convergence of the stochastic recursion to the limiting deterministic recursion as $b \rightarrow \infty$; (ii) deriving the critical fidelity threshold $\rho_c(r)$; and (iii) characterizing the long-run behavior of the limiting recursion for all initial conditions $\theta_0 \in (0, 1)$.

Part I: Convergence to the limiting recursion as $b \rightarrow \infty$. Let $(\theta_n^{(b)})_{n \geq 0}$ denote the sequence generated by the stochastic recursion (7) with batch size b , and let $(\theta_n)_{n \geq 0}$ denote the solution of the limiting recursion (11) with the same initial condition θ_0 .

For each $n \geq 0$, define the estimation error $\varepsilon_n^{(b)} := \bar{D}_n^{(b)} - \Delta(\theta_n^{(b)})$. By Lemma 1, conditional on the history \mathcal{H}_n , the estimator $\bar{D}_n^{(b)}$ is an unbiased estimator of $\Delta(\theta_n^{(b)})$ with variance $\text{Var}(\bar{D}_n^{(b)} | \mathcal{H}_n) = O(1/b)$. More precisely, for any fixed $\rho \in (1/2, 1)$, there exists a constant $C_{\rho} < \infty$ such that $\text{Var}(\bar{D}_n^{(b)} | \mathcal{H}_n) \leq C_{\rho}/b$ uniformly in n and $\theta_n^{(b)} \in (0, 1)$.

We now show that $\theta_n^{(b)} \rightarrow \theta_n$ almost surely as $b \rightarrow \infty$, uniformly over any finite horizon. Fix $N < \infty$. The stochastic recursion can be written as

$$z_{n+1}^{(b)} = z_n^{(b)} + \gamma_n [\Delta(\theta_n^{(b)}) + \varepsilon_n^{(b)}],$$

while the limiting recursion satisfies

$$z_{n+1} = z_n + \gamma_n \Delta(\theta_n).$$

Taking differences and using the global Lipschitz continuity of $h(z) := \Delta(\sigma(z))$ from Lemma 2, we obtain

$$|z_{n+1}^{(b)} - z_{n+1}| \leq |z_n^{(b)} - z_n| + \gamma_n L |z_n^{(b)} - z_n| + \gamma_n |\varepsilon_n^{(b)}|,$$

where L is a global Lipschitz constant of h .

Iterating this bound and applying the discrete Gronwall inequality yields

$$\max_{0 \leq n \leq N} |z_n^{(b)} - z_n| \leq \exp\left(L \sum_{k=0}^{N-1} \gamma_k\right) \sum_{k=0}^{N-1} \gamma_k |\varepsilon_k^{(b)}|.$$

To upgrade to almost sure convergence in b , we work under a natural coupling where, at each step k , the batch of size b is the prefix of an infinite i.i.d. stream of interaction rounds. We then use the uniform boundedness of the per-round estimator. For fixed $\rho \in (1/2, 1)$, Lemma 1 implies that $D(\theta)$ is uniformly bounded over $\theta \in [0, 1]$, so there exists $B_\rho < \infty$ such that $|D(\theta)| \leq B_\rho$ almost surely for all $\theta \in [0, 1]$. Consequently, conditional on \mathcal{H}_k , the estimation error $\varepsilon_k^{(b)}$ is an average of b independent, mean-zero, bounded random variables, and Hoeffding's inequality yields a constant $c_\rho > 0$ such that for any $\delta > 0$,

$$\mathbb{P}\left(|\varepsilon_k^{(b)}| > \delta \mid \mathcal{H}_k\right) \leq 2 \exp(-c_\rho b \delta^2).$$

Taking expectations and applying a union bound over $k = 0, 1, \dots, N-1$ gives

$$\mathbb{P}\left(\max_{0 \leq k \leq N-1} |\varepsilon_k^{(b)}| > b^{-1/3}\right) \leq 2N \exp(-c_\rho b^{1/3}).$$

Since $\sum_{b=1}^{\infty} 2N \exp(-c_\rho b^{1/3}) < \infty$, the Borel–Cantelli lemma implies that $\max_{0 \leq k \leq N-1} |\varepsilon_k^{(b)}| \leq b^{-1/3}$ eventually almost surely as $b \rightarrow \infty$. On this event,

$$\max_{0 \leq n \leq N} |z_n^{(b)} - z_n| \leq \exp\left(L \sum_{k=0}^{N-1} \gamma_k\right) b^{-1/3} \sum_{k=0}^{N-1} \gamma_k \xrightarrow{b \rightarrow \infty} 0$$

almost surely. Since σ is Lipschitz with constant $1/4$, this implies $\max_{0 \leq n \leq N} |\theta_n^{(b)} - \theta_n| \rightarrow 0$ almost surely. Since N was arbitrary, a diagonalization argument yields almost-sure convergence uniformly on finite horizons.

Part II: Derivation of the critical fidelity threshold. By Proposition 1, the sign of $\Delta(\theta)$ on the interior $(0, 1)$ is determined by the statistic $s(\rho, r)$ defined in (12). The critical case, where $\Delta(\theta) = 0$ has a unique interior solution at $\theta = 1/2$, occurs when $s(\rho, r) = 1$, i.e.,

$$\frac{2(2-r)\rho(1-\rho)}{(r-1)(2\rho-1)^2} = 1.$$

Cross-multiplying and rearranging yields the quadratic equation

$$2(2-r)\rho(1-\rho) = (r-1)(2\rho-1)^2.$$

Expanding both sides:

$$\text{LHS} = 2(2-r)\rho - 2(2-r)\rho^2 = (4-2r)\rho - (4-2r)\rho^2,$$

$$\text{RHS} = (r-1)(4\rho^2 - 4\rho + 1) = (4r-4)\rho^2 - (4r-4)\rho + (r-1).$$

Collecting terms:

$$0 = [(4r-4) + (4-2r)]\rho^2 - [(4r-4) + (4-2r)]\rho + (r-1).$$

Simplifying the coefficient: $(4r-4) + (4-2r) = 2r$, so

$$2r\rho^2 - 2r\rho + (r-1) = 0.$$

Dividing by $2r$ and applying the quadratic formula:

$$\rho = \frac{1 \pm \sqrt{1 - 2(r-1)/r}}{2} = \frac{1 \pm \sqrt{(2-r)/r}}{2}.$$

Since $\rho \in (1/2, 1]$ and $r \in (1, 2)$ implies $(2-r)/r \in (0, 1)$, we have $\sqrt{(2-r)/r} \in (0, 1)$. The solution $\rho_- = (1 - \sqrt{(2-r)/r})/2 < 1/2$ lies outside the feasible range, so the unique critical threshold is

$$\rho_c(r) = \frac{1 + \sqrt{(2-r)/r}}{2}.$$

Part III: Long-run behavior of the limiting recursion. We now characterize the convergence of $(\theta_n)_{n \geq 0}$ as $n \rightarrow \infty$ for each regime of ρ .

Write $h(z) \triangleq \Delta(\sigma(z))$, so the limiting recursion is $z_{n+1} = z_n + \gamma_n h(z_n)$ with $\theta_n = \sigma(z_n)$. Under our step-size choice, $0 < \gamma_n \leq \eta \leq 1$.

We first record a monotonicity property that prevents spurious basin crossings in the deterministic recursion. For $\rho \in (1/2, 1)$, one can simplify the payoff difference to

$$\Delta(\theta) = 2(r-1) - \frac{r\rho(1-\rho)}{p_H(\theta)p_L(\theta)}, \quad p_H(\theta) = (1-\rho) + (2\rho-1)\theta, \quad p_L(\theta) = 1 - p_H(\theta).$$

Differentiating and using $\sigma'(z) = \sigma(z)(1-\sigma(z))$ yields, for $\rho \in (1/2, 1)$,

$$|h'(z)| = |\Delta'(\sigma(z))| \sigma'(z) = r \frac{t(z) |2\sigma(z) - 1|}{(1+t(z))^2} \leq \frac{r}{4} \quad \text{for all } z \in \mathbb{R},$$

where $t(z) \triangleq \frac{(2\rho-1)^2 \sigma(z)(1-\sigma(z))}{\rho(1-\rho)}$ and we used $x/(1+x)^2 \leq 1/4$ for all $x \geq 0$. When $\rho = 1$, we have $h(z) \equiv 2r - 2$, so $|h'(z)| = 0$ and the same bound holds. Therefore h is globally Lipschitz with constant $L := r/4 < 1/2$. For each n , define the update map $T_n(z) := z + \gamma_n h(z)$. For any $z \leq z'$,

$$T_n(z') - T_n(z) = (z' - z) + \gamma_n (h(z') - h(z)) \geq (1 - \gamma_n L)(z' - z) \geq 0,$$

so T_n is increasing. In particular, if $h(\bar{z}) = 0$ and $z_n \geq \bar{z}$, then $z_{n+1} = T_n(z_n) \geq T_n(\bar{z}) = \bar{z}$.

Case 1: Low-fidelity regime ($\rho < \rho_c(r)$).

By Proposition 1, $s(\rho, r) > 1$ implies $\Delta(\theta) < 0$ for all $\theta \in (0, 1)$. The limiting recursion satisfies

$$z_{n+1} = z_n + \gamma_n \Delta(\theta_n) < z_n,$$

so $(z_n)_{n \geq 0}$ is strictly decreasing. Since $\Delta(\theta)$ is bounded away from zero on any compact subset of $(0, 1)$ and $\sum_n \gamma_n = \infty$, we have $z_n \rightarrow -\infty$ and hence $\theta_n = \sigma(z_n) \rightarrow 0$.

Case 2: Critical regime ($\rho = \rho_c(r)$).

Here $s(\rho, r) = 1$, so $\Delta(1/2) = 0$ and $\Delta(\theta) < 0$ for all $\theta \in (0, 1) \setminus \{1/2\}$.

If $\theta_0 = 1/2$, then $\Delta(\theta_0) = 0$ implies $z_1 = z_0 + \gamma_0 \cdot 0 = z_0$, and by induction $z_n = z_0$ for all n , so $\theta_n \equiv 1/2$.

If $\theta_0 < 1/2$ (equivalently, $z_0 < 0$), then $\Delta(\theta_0) < 0$, so $z_1 < z_0 < 0$. Since $\Delta(\theta) < 0$ for all $\theta \neq 1/2$, the sequence (z_n) remains negative and strictly decreasing. By the same argument as Case 1, $z_n \rightarrow -\infty$ and $\theta_n \rightarrow 0$.

If $\theta_0 > 1/2$ (equivalently, $z_0 > 0$), then $\Delta(\theta_0) < 0$, so $z_1 < z_0$. Since $h(0) = \Delta(1/2) = 0$ and each T_n is increasing, $z_n \geq 0$ implies $z_{n+1} = T_n(z_n) \geq T_n(0) = 0$. Thus $z_n \geq 0$ for all n . Moreover, $h(z) < 0$ for all $z > 0$, so (z_n) is strictly decreasing and bounded below by 0, hence $z_n \rightarrow z^*$ for some $z^* \geq 0$. If $z^* > 0$, then $h(z^*) < 0$ and by continuity there exists $c > 0$ such that $h(z) \leq -c$ for all z in a neighborhood of z^* . For all n large enough we then have $z_{n+1} \leq z_n - c\gamma_n$, which implies $z_n \rightarrow -\infty$ since $\sum_n \gamma_n = \infty$, a contradiction. Therefore $z^* = 0$ and $\theta_n = \sigma(z_n) \rightarrow 1/2$.

Case 3: High-fidelity regime ($\rho_c(r) < \rho < 1$).

By Proposition 1, $s(\rho, r) < 1$ implies the existence of thresholds $\theta_-(\rho, r) < 1/2 < \theta_+(\rho, r)$ such that

$$\Delta(\theta) \begin{cases} < 0, & \theta \in (0, \theta_-), \\ = 0, & \theta \in \{\theta_-, \theta_+\}, \\ > 0, & \theta \in (\theta_-, \theta_+), \\ < 0, & \theta \in (\theta_+, 1). \end{cases}$$

Subcase 3(a): $\theta_0 \in (0, \theta_-)$. Then $z_0 < z_- := \log(\theta_-/(1 - \theta_-))$ and $h(z) < 0$ for all $z < z_-$. Hence (z_n) is strictly decreasing and $z_n \rightarrow -\infty$, so $\theta_n \rightarrow 0$.

Subcase 3(b): $\theta_0 \in (\theta_-, 1)$. Then $z_0 > z_-$, and since $h(z_-) = 0$ and T_n is increasing, we have $z_n > z_-$ for all n . Let $z_+ := \log(\theta_+/(1 - \theta_+))$. The sign pattern of Δ implies $h(z) > 0$ for $z \in (z_-, z_+)$ and $h(z) < 0$ for $z > z_+$. Therefore, if $z_n \leq z_+$ then $z_{n+1} \geq z_n$, and if $z_n \geq z_+$ then $z_{n+1} \leq z_n$. In either case, the recursion moves toward z_+ .

If z_n crosses z_+ only finitely many times, then eventually it stays on one side of z_+ and is monotone, hence it converges to some limit z^* . If $h(z^*) \neq 0$, then by continuity there exists $c > 0$

such that $|h(z_n)| \geq c$ for all n large enough, which implies $|z_{n+1} - z_n| = \gamma_n |h(z_n)| \geq c\gamma_n$ eventually. Since $\sum_n \gamma_n = \infty$, this contradicts convergence of (z_n) . Therefore $h(z^*) = 0$, and given $z_n > z_-$ for all n this forces $z^* = z_+$.

If z_n crosses z_+ infinitely many times, let $H := \sup_{z \in \mathbb{R}} |h(z)| < \infty$. At each crossing between n and $n+1$, the point z_+ lies between z_n and z_{n+1} , so

$$\max\{|z_n - z_+|, |z_{n+1} - z_+|\} \leq |z_{n+1} - z_n| = \gamma_n |h(z_n)| \leq \gamma_n H.$$

Since $\gamma_n \rightarrow 0$, the distance to z_+ at crossing times tends to 0. Between crossings, the recursion is monotone and stays between z_+ and the most recent crossing value, so the distance to z_+ is bounded by the corresponding crossing distance. Therefore $|z_n - z_+| \rightarrow 0$ and $z_n \rightarrow z_+$.

In both cases, $z_n \rightarrow z_+$ and therefore $\theta_n = \sigma(z_n) \rightarrow \theta_+(\rho, r)$.

Case 4: Perfect-fidelity regime ($\rho = 1$).

When $\rho = 1$, only the outcomes (H, H) and (L, L) occur (since recommendations match the latent mode with probability one). The conditional payoff difference becomes

$$\Delta(\theta) = \mathbb{E}[\Pi | S = H] - \mathbb{E}[\Pi | S = L] = 2r - 2 > 0$$

for all $\theta \in (0, 1)$, since $r > 1$.

Thus $z_{n+1} = z_n + \gamma_n(2r - 2) > z_n$ for all n , and since $\sum_n \gamma_n = \infty$, we have $z_n \rightarrow +\infty$ and $\theta_n \rightarrow 1$.

This completes the proof of Proposition 2. □

Proof of Proposition 3. Recall the stochastic approximation form (15):

$$z_{n+1} = z_n + \gamma_n(\Delta(\theta_n) + M_{n+1}), \quad \theta_n = \sigma(z_n).$$

The step sizes $\gamma_n = \eta/(n+1)^\alpha$ satisfy $\sum_n \gamma_n = \infty$ and $\sum_n \gamma_n^2 < \infty$ because $\alpha \in (1/2, 1]$. For fixed $\rho \in (1/2, 1)$, Lemma 1 implies $\mathbb{E}[M_{n+1} | \mathcal{H}_n] = 0$ and $\sup_n \mathbb{E}[M_{n+1}^2] < \infty$.

Step 1: Noise summability. Define the martingale partial sums $W_n \triangleq \sum_{k=0}^{n-1} \gamma_k M_{k+1}$. Since $\sum_k \gamma_k^2 < \infty$ and the conditional second moments of M_{k+1} are uniformly bounded, (W_n) is L^2 bounded and hence converges almost surely to a finite limit W_∞ (Durrett 2019, Theorem 5.4.9). Consequently,

$$z_n = z_0 + \sum_{k=0}^{n-1} \gamma_k \Delta(\theta_k) + W_n. \tag{A.7}$$

Step 2: Excluding $\theta_n \rightarrow 1$. Because $\rho < 1$, Proposition 1 implies $\Delta(1) < 0$. By continuity of Δ on $[0, 1]$, there exist $\bar{\theta} \in (0, 1)$ and $c_1 > 0$ such that $\Delta(\theta) \leq -c_1$ for all $\theta \in [\bar{\theta}, 1]$. If $\theta_n \rightarrow 1$, then $\theta_n \geq \bar{\theta}$ for all large n , and (A.7) would imply

$$z_n \leq z_0 - c_1 \sum_{k=0}^{n-1} \gamma_k + W_n \rightarrow -\infty,$$

which contradicts $\theta_n = \sigma(z_n) \rightarrow 1$. Therefore, $\mathbb{P}(\theta_n \rightarrow 1) = 0$.

Step 3: Convergence to ODE equilibria. Using the first-order expansion (8) and the definition of M_{n+1} , we can write

$$\theta_{n+1} = \theta_n + \gamma_n \left(\theta_n(1 - \theta_n)\Delta(\theta_n) + \theta_n(1 - \theta_n)M_{n+1} \right) + r_{n+1}, \quad (\text{A.8})$$

where the remainder satisfies $|r_{n+1}| \leq C\gamma_n^2$ for a constant C that depends only on (ρ, r) and the payoff bounds. Since $\sum_n \gamma_n^2 < \infty$, we also have $\sum_n |r_{n+1}| < \infty$. The drift $g(\theta) \triangleq \theta(1 - \theta)\Delta(\theta)$ is continuously differentiable on $[0, 1]$ for $\rho \in (1/2, 1)$, hence Lipschitz. Since $\theta_n \in (0, 1)$ is bounded, standard ODE-method results for stochastic approximation applied to (A.8) imply that θ_n converges almost surely to an equilibrium of the ODE (10) (Borkar 2008, Benaïm 1999).

Step 4: Identifying the possible limits. The equilibria of (10) are $\theta \in \{0, 1\}$ and any interior θ^* satisfying $\Delta(\theta^*) = 0$. Proposition 1 characterizes the interior zeros.

1. If $\rho \in (1/2, \rho_c(r))$, then $\Delta(\theta) < 0$ for all $\theta \in (0, 1)$, so the only equilibria are $\theta \in \{0, 1\}$. Since $\mathbb{P}(\theta_n \rightarrow 1) = 0$ by Step 2, we obtain $\theta_n \rightarrow 0$ almost surely.
2. If $\rho = \rho_c(r)$, then $\Delta(\theta) = 0$ if and only if $\theta = 1/2$, so the equilibria are $\theta \in \{0, 1/2, 1\}$. Step 2 rules out $\theta_n \rightarrow 1$, hence $\theta_\infty \in \{0, 1/2\}$ almost surely.
3. If $\rho \in (\rho_c(r), 1)$, then $\Delta(\theta) = 0$ if and only if $\theta \in \{\theta_-(\rho, r), \theta_+(\rho, r)\}$, so the equilibria are $\theta \in \{0, \theta_-, \theta_+, 1\}$. Step 2 rules out $\theta_n \rightarrow 1$. Moreover, $\theta_-(\rho, r)$ is linearly unstable for (10), and the noise in (A.8) is nondegenerate on any neighborhood of θ_- for fixed b . Standard nonconvergence results for stochastic approximation then imply $\mathbb{P}(\theta_n \rightarrow \theta_-) = 0$, so $\theta_\infty \in \{0, \theta_+(\rho, r)\}$ almost surely.

□

Proof of Proposition 4. Throughout, write $h(z) \triangleq \Delta(\sigma(z))$ so that the stochastic recursion in log-odds form is

$$z_{n+1} = z_n + \gamma_n (h(z_n) + M_{n+1}), \quad \theta_n = \sigma(z_n),$$

where $M_{n+1} \triangleq \bar{D}_n^{(b)} - \Delta(\theta_n)$ is a martingale-difference term with $\mathbb{E}[M_{n+1} | \mathcal{H}_n] = 0$.

Part (i). Fix $T > 0$ and let $N(T) \triangleq \min\{n : \sum_{k=0}^{n-1} \gamma_k \geq T\}$. Let z_n^{\det} denote the deterministic recursion (11) and write $\theta_n^{\det} \triangleq \sigma(z_n^{\det})$. Define the error $e_n \triangleq z_n - z_n^{\det}$, which satisfies

$$e_{n+1} = e_n + \gamma_n (h(z_n) - h(z_n^{\det})) + \gamma_n M_{n+1}.$$

Define the martingale partial sums $W_m \triangleq \sum_{k=0}^{m-1} \gamma_k M_{k+1}$, with $W_0 = 0$, and set $u_n \triangleq e_n - W_n$. Then

$$u_{n+1} = u_n + \gamma_n (h(z_n) - h(z_n^{\det})).$$

As shown in the proof of Proposition 2, h is globally Lipschitz on \mathbb{R} with some constant $L < \infty$. Let $W_* \triangleq \max_{0 \leq m \leq N(T)} |W_m|$. For $n \leq N(T)$,

$$|u_{n+1}| \leq |u_n| + \gamma_n L |e_n| = |u_n| + \gamma_n L |u_n + W_n| \leq (1 + L\gamma_n) |u_n| + L\gamma_n W_*.$$

Iterating this inequality and using $\sum_{k=0}^{N(T)-1} \gamma_k \leq T + \gamma_0 \leq T + 1$ yields

$$\max_{0 \leq n \leq N(T)} |u_n| \leq e^{L(T+1)} L(T+1) W_*.$$

Since $e_n = u_n + W_n$, we obtain

$$\max_{0 \leq n \leq N(T)} |e_n| \leq (1 + e^{L(T+1)} L(T+1)) W_*.$$

Because $\bar{D}_n^{(b)}$ is a batch average of bounded per-round statistics (Lemma 1), there exists $V < \infty$ depending only on (ρ, r) such that

$$\mathbb{E}[M_{n+1}^2 | \mathcal{H}_n] \leq \frac{V}{b} \quad \text{a.s. for all } n.$$

Therefore,

$$\mathbb{E}[W_{N(T)}^2] = \sum_{k=0}^{N(T)-1} \gamma_k^2 \mathbb{E}[M_{k+1}^2] \leq \frac{V}{b} \sum_{k=0}^{N(T)-1} \gamma_k^2.$$

By Doob's L^2 maximal inequality,

$$\mathbb{P}(W_* > \xi) \leq \frac{4\mathbb{E}[W_{N(T)}^2]}{\xi^2} \leq \frac{4V \sum_{k=0}^{N(T)-1} \gamma_k^2}{b \xi^2}.$$

Using that σ is $1/4$ Lipschitz, we have $|\theta_n - \theta_n^{\det}| \leq \frac{1}{4}|e_n|$, hence

$$\mathbb{P}\left(\max_{0 \leq n \leq N(T)} |\theta_n - \theta_n^{\det}| > \varepsilon\right) \leq \frac{C(T, \rho, r, \alpha, \eta)}{b \varepsilon^2}.$$

Passing from discrete time to the interpolations $\bar{\theta}(t)$ and $\theta^{\det}(t)$ on $t \in [0, T]$ changes only constants, because the interpolation error is $O(\max_{n \leq N(T)} \gamma_n)$ and does not depend on b . This yields the displayed bound in Part (i) and the $O_p(1/\sqrt{b})$ statement follows.

Part (ii). Fix $\delta \in (0, 1/2)$ and recall

$$K_+(\delta) \triangleq [\theta_- + \delta, 1 - \delta], \quad K_-(\delta) \triangleq [\delta, \theta_- - \delta].$$

Write

$$z_- := \log\left(\frac{\theta_-}{1 - \theta_-}\right), \quad z_+ := \log\left(\frac{\theta_+}{1 - \theta_+}\right).$$

By Proposition 3, in this regime θ_n converges almost surely, and the only possible limits are 0 and $\theta_+(\rho, r)$.

Step 1: A maximal inequality for the weighted martingale noise. Write the batch estimator as an average of b i.i.d. per-round scores. Define

$$\tilde{D}_n^{(\ell)} \triangleq \frac{1}{2} \sum_{i=1}^2 D_i^{(\ell)}(\theta_n), \quad \ell = 1, \dots, b,$$

so that $\overline{D}_n^{(b)} = \frac{1}{b} \sum_{\ell=1}^b \tilde{D}_n^{(\ell)}$. Conditional on \mathcal{H}_n , the random variables $(\tilde{D}_n^{(\ell)})_{\ell=1}^b$ are i.i.d. with mean $\Delta(\theta_n)$. By Lemma 1, there exist constants $\underline{D} < \overline{D}$ depending only on (ρ, r) such that $\underline{D} \leq \tilde{D}_n^{(\ell)} \leq \overline{D}$ almost surely for all n and ℓ . Consequently, Hoeffding's lemma implies that for all $\lambda \in \mathbb{R}$,

$$\mathbb{E}[\exp(\lambda M_{n+1}) \mid \mathcal{H}_n] \leq \exp\left(\frac{\lambda^2 V_\star}{2b}\right), \quad V_\star := \left(\frac{\overline{D} - \underline{D}}{2}\right)^2. \quad (\text{A.9})$$

Define the weighted martingale

$$W_n := \sum_{k=0}^{n-1} \gamma_k M_{k+1}, \quad W_0 = 0, \quad S_2 := \sum_{k=0}^{\infty} \gamma_k^2 < \infty.$$

Fix $\lambda > 0$ and define

$$\mathcal{E}_n(\lambda) := \exp\left(\lambda W_n - \frac{\lambda^2 V_\star}{2b} \sum_{k=0}^{n-1} \gamma_k^2\right).$$

Using (A.9) and iterated expectations, $(\mathcal{E}_n(\lambda), \mathcal{H}_n)$ is a nonnegative supermartingale with $\mathbb{E}[\mathcal{E}_0(\lambda)] = 1$. By Ville's inequality,

$$\mathbb{P}\left(\sup_{n \geq 0} W_n \geq t\right) \leq \exp\left(-\lambda t + \frac{\lambda^2 V_\star S_2}{2b}\right).$$

Optimizing over λ yields

$$\mathbb{P}\left(\sup_{n \geq 0} W_n \geq t\right) \leq \exp\left(-\frac{b t^2}{2V_\star S_2}\right), \quad \mathbb{P}\left(\inf_{n \geq 0} W_n \leq -t\right) \leq \exp\left(-\frac{b t^2}{2V_\star S_2}\right).$$

Therefore, for every $t > 0$,

$$\mathbb{P}\left(\sup_{n \geq 0} |W_n| \geq t\right) \leq 2 \exp\left(-\frac{b t^2}{2V_\star S_2}\right). \quad (\text{A.10})$$

Step 2: A deterministic barrier lemma. Define the down-crossing and up-crossing times of the unstable log-odds threshold z_- ,

$$\tau_- := \inf\{n \geq 0 : z_n \leq z_-\}, \quad \tau_+ := \inf\{n \geq 0 : z_n \geq z_-\}.$$

Claim (Barrier bound for separatrix crossings). Fix $\delta \in (0, 1/2)$ such that $\theta_- - \delta$ and $\theta_- + \delta$ lie in $(0, 1)$, and define

$$z_\delta^+ := \log\left(\frac{\theta_- + \delta}{1 - (\theta_- + \delta)}\right), \quad z_\delta^- := \log\left(\frac{\theta_- - \delta}{1 - (\theta_- - \delta)}\right), \quad z_{\text{mid}} := \frac{z_- + z_+}{2}, \quad \underline{z}_\delta := z_\delta^+ \wedge z_{\text{mid}}.$$

(a) If $z_0 \geq z_\delta^+$ and $\tau_- < \infty$, then $\sup_{n \geq 0} |W_n| \geq (\underline{z}_\delta - z_-)/2$.

(b) If $z_0 \leq z_\delta^-$ and $\tau_+ < \infty$, then $\sup_{n \geq 0} |W_n| \geq (z_- - z_\delta^-)/2$.

Proof. Part (a). Assume $z_0 \geq z_\delta^+$ and $\tau_- < \infty$. Define the last time before τ_- at which the process is at or above \underline{z}_δ ,

$$\tau_\delta := \sup\{n \leq \tau_- : z_n \geq \underline{z}_\delta\}.$$

Then $z_{\tau_\delta} \geq \underline{z}_\delta$ and $z_{\tau_\delta+1} < \underline{z}_\delta$.

If $z_{\tau_\delta} \leq z_+$, then for every k with $\tau_\delta \leq k < \tau_-$ we have $z_- < z_k \leq z_+$ and hence $h(z_k) \geq 0$. Writing $z_n = z_0 + \sum_{k=0}^{n-1} \gamma_k h(z_k) + W_n$ gives

$$z_{\tau_-} = z_{\tau_\delta} + \sum_{k=\tau_\delta}^{\tau_- - 1} \gamma_k h(z_k) + (W_{\tau_-} - W_{\tau_\delta}).$$

On $\{\tau_- < \infty\}$, the middle term is nonnegative, so

$$W_{\tau_-} - W_{\tau_\delta} \leq z_{\tau_-} - z_{\tau_\delta} \leq z_- - \underline{z}_\delta = -(\underline{z}_\delta - z_-).$$

If $\sup_n |W_n| < (\underline{z}_\delta - z_-)/2$, then $W_{\tau_\delta} \leq \sup_n |W_n| < (\underline{z}_\delta - z_-)/2$ and hence

$$W_{\tau_-} \leq W_{\tau_\delta} - (\underline{z}_\delta - z_-) < \frac{\underline{z}_\delta - z_-}{2} - (\underline{z}_\delta - z_-) = -\frac{\underline{z}_\delta - z_-}{2},$$

which contradicts $\sup_n |W_n| < (\underline{z}_\delta - z_-)/2$.

If instead $z_{\tau_\delta} > z_+$, define $T_n(z) := z + \gamma_n h(z)$. As shown in the proof of Proposition 2, $|h'(z)| \leq r/4$ for all z and since $\gamma_n \leq 1$ this implies T_n is increasing. Because $T_{\tau_\delta}(z_+) = z_+$ and $z_{\tau_\delta} \geq z_+$, we obtain $T_{\tau_\delta}(z_{\tau_\delta}) \geq z_+$. Therefore,

$$|W_{\tau_\delta+1} - W_{\tau_\delta}| = |z_{\tau_\delta+1} - T_{\tau_\delta}(z_{\tau_\delta})| \geq z_+ - \underline{z}_\delta.$$

Since $\underline{z}_\delta \leq z_{\text{mid}} = (z_- + z_+)/2$, we have $z_+ - \underline{z}_\delta \geq \underline{z}_\delta - z_-$. Using $|W_{\tau_\delta+1} - W_{\tau_\delta}| \leq |W_{\tau_\delta+1}| + |W_{\tau_\delta}| \leq 2 \sup_n |W_n|$ yields $\sup_n |W_n| \geq (\underline{z}_\delta - z_-)/2$.

Part (b). Assume $z_0 \leq z_\delta^-$ and $\tau_+ < \infty$. Define the last time before τ_+ at which the process is at or below z_δ^- ,

$$\widehat{\tau}_\delta := \sup\{n \leq \tau_+ : z_n \leq z_\delta^-\}.$$

Then $z_{\widehat{\tau}_\delta} \leq z_\delta^-$, and for every k with $\widehat{\tau}_\delta \leq k < \tau_+$ we have $z_\delta^- < z_k < z_-$, hence $h(z_k) \leq 0$. Decomposing again,

$$z_{\tau_+} = z_{\widehat{\tau}_\delta} + \sum_{k=\widehat{\tau}_\delta}^{\tau_+-1} \gamma_k h(z_k) + (W_{\tau_+} - W_{\widehat{\tau}_\delta}),$$

and the middle term is nonpositive, so

$$W_{\tau_+} - W_{\widehat{\tau}_\delta} \geq z_{\tau_+} - z_{\widehat{\tau}_\delta} \geq z_- - z_\delta^-.$$

If $\sup_n |W_n| < (z_- - z_\delta^-)/2$, then $W_{\widehat{\tau}_\delta} \geq -\sup_n |W_n| > -(z_- - z_\delta^-)/2$ and thus

$$W_{\tau_+} \geq W_{\widehat{\tau}_\delta} + (z_- - z_\delta^-) > -\frac{z_- - z_\delta^-}{2} + (z_- - z_\delta^-) = \frac{z_- - z_\delta^-}{2},$$

contradicting $\sup_n |W_n| < (z_- - z_\delta^-)/2$. \square

Step 3: Conclude the exponential bounds. Fix $\delta \in (0, 1/2)$.

If $\theta_0 \in K_+(\delta)$ then $z_0 \geq z_\delta^+$. On the event $\{\theta_n \rightarrow 0\}$ we have $z_n \rightarrow -\infty$, hence $\tau_- < \infty$. Therefore, using Step 2(a) and (A.10),

$$1 - p_+(b, \theta_0) = \mathbb{P}(\theta_n \rightarrow 0 \mid \theta_0) \leq \mathbb{P}\left(\sup_{n \geq 0} |W_n| \geq \frac{z_\delta - z_-}{2} \mid \theta_0\right) \leq 2 \exp\left(-\frac{b(z_\delta - z_-)^2}{8V_\star S_2}\right).$$

Similarly, if $\theta_0 \in K_-(\delta)$ then $z_0 \leq z_\delta^-$. On the event $\{\theta_n \rightarrow \theta_+\}$ we have $z_n \rightarrow z_+ > z_-$, hence $\tau_+ < \infty$.

Step 2(b) and (A.10) give

$$p_+(b, \theta_0) \leq \mathbb{P}\left(\sup_{n \geq 0} |W_n| \geq \frac{z_- - z_\delta^-}{2} \mid \theta_0\right) \leq 2 \exp\left(-\frac{b(z_- - z_\delta^-)^2}{8V_\star S_2}\right).$$

Finally, note that

$$z_\delta^+ - z_- = \int_{\theta_-}^{\theta_- + \delta} \frac{d\theta}{\theta(1-\theta)} \geq 4\delta, \quad z_- - z_\delta^- = \int_{\theta_- - \delta}^{\theta_-} \frac{d\theta}{\theta(1-\theta)} \geq 4\delta,$$

and $z_\delta - z_- = (z_\delta^+ - z_-) \wedge ((z_+ - z_-)/2)$. This implies the displayed bounds in Part (ii) after absorbing constants into c_δ and C_δ . For any fixed $\theta_0 \neq \theta_-$, choose $\delta > 0$ such that $\theta_0 \in K_+(\delta)$ when $\theta_0 > \theta_-$ and $\theta_0 \in K_-(\delta)$ when $\theta_0 < \theta_-$. Letting $b \rightarrow \infty$ then yields $\lim_{b \rightarrow \infty} p_+(b, \theta_0) = \mathbb{1}\{\theta_0 > \theta_-\}$.

Part (iii). Fix $\epsilon \in (0, 1/2)$ and $\delta_0 \in (0, 1/2)$ with $\theta_- \in (\delta_0, 1 - \delta_0)$. Set

$$\kappa_{\delta_0} := \min \left\{ 4, \frac{z_+ - z_-}{2\delta_0} \right\}.$$

Let $\theta_0 \in [\delta_0, 1 - \delta_0]$ and define $\delta := \min\{\frac{1}{2}|\theta_0 - \theta_-|, \delta_0\}$. If $\theta_0 = \theta_-$, the conclusion is immediate, so assume $\theta_0 \neq \theta_-$. If $\theta_0 > \theta_-$ then $\theta_0 \in K_+(\delta)$, and if $\theta_0 < \theta_-$ then $\theta_0 \in K_-(\delta)$.

For $\delta \leq \delta_0$ we have

$$z_\delta - z_- = (z_\delta^+ - z_-) \wedge \left(\frac{z_+ - z_-}{2} \right) \geq \kappa_{\delta_0} \delta, \quad z_- - z_\delta^- \geq 4\delta \geq \kappa_{\delta_0} \delta.$$

Therefore, by the bounds established in Part (ii), for all $b \geq 1$,

$$p_+(b, \theta_0) \in (\epsilon, 1 - \epsilon) \implies \epsilon \leq 2 \exp \left(-\frac{\kappa_{\delta_0}^2}{8V_\star S_2} b \delta^2 \right).$$

Rearranging yields

$$\delta^2 \leq \frac{8V_\star S_2}{\kappa_{\delta_0}^2 b} \log \left(\frac{2}{\epsilon} \right).$$

Define

$$A := \sqrt{\frac{8V_\star S_2}{\kappa_{\delta_0}^2} \log \left(\frac{2}{\epsilon} \right)}.$$

Then $\delta \leq A/\sqrt{b}$. If $|\theta_0 - \theta_-| \leq 2\delta_0$, we have $\delta = \frac{1}{2}|\theta_0 - \theta_-|$, so $|\theta_0 - \theta_-| = 2\delta \leq 2A/\sqrt{b}$. If instead $|\theta_0 - \theta_-| > 2\delta_0$, we have $\delta = \delta_0$, so $\delta_0 \leq A/\sqrt{b}$ and hence $b \leq A^2/\delta_0^2$. Since $|\theta_0 - \theta_-| \leq 1$, this implies $|\theta_0 - \theta_-| \leq (A/\delta_0)/\sqrt{b}$. Taking $K := A/\delta_0$ completes the proof. \square